

See discussions, stats, and author profiles for this publication at: <https://www.researchgate.net/publication/384972647>

Free Radical Polymerizations: LDPE and EVA

Chapter · August 2023

DOI: 10.1002/9783527843831.ch4

CITATIONS

13

READS

244

2 authors, including:



Niket Sharma

Aspen Technology, Inc.

20 PUBLICATIONS 278 CITATIONS

SEE PROFILE

Free Radical Polymerizations: LDPE and EVA

Y.A. Liu and Niket Sharma

Department of Chemical Engineering, Virginia Polytechnic Institute and State University,
Blacksburg, Virginia 24061, U.S.A

Abstract

This chapter provides an in-depth exploration of the modeling of high-pressure manufacturing processes for low-density polyethylene (LDPE) and polyethylene-vinyl acetate (EVA) copolymer, utilizing free radical polymerization in stirred autoclave and tubular reactors. The chapter integrates conceptual development, modeling methodologies, illustrative examples, and practical workshops, offering a comprehensive learning experience.

Key topics include the kinetics of free radical polymerization and copolymerization, the selection of appropriate thermodynamic methods, and the estimation of essential property parameters for simulating polyolefin processes. A novel contribution is the methodology for estimating kinetic parameters based on plant data, enabling the development of accurate simulation and optimization models for commercial polyolefin processes.

Hands-on workshops are incorporated throughout the chapter to simulate both autoclave and tubular reactor processes, emphasizing practical applications in high-pressure LDPE and EVA copolymerization processes. This chapter serves as a critical resource for professionals and researchers seeking to optimize polyolefin production through advanced modeling and simulation techniques. The integration of theoretical and practical elements sets the foundation for enhanced process design and optimization.

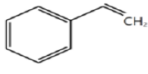
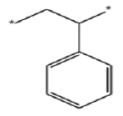
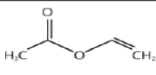
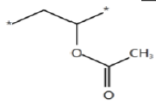
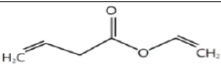
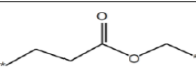
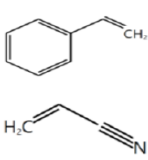
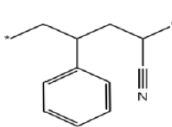
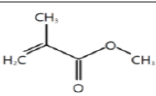
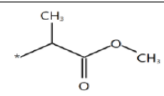
This is a preprint version of a chapter from our book - *Integrated Process Modeling, Advanced Control and Data Analytics for Optimizing Polyolefin Manufacturing* [39,43]. Please cite the original work if referenced

4.1 Polymers by Free Radical Polymerization

We cover conceptual development, modeling methodology, illustrative examples, and hands-on workshops. Section 4.1 introduces polymers by free radical polymerization. Section 4.2 covers the kinetics of free radical polymerization and copolymerization. Section 4.3 explains the selection of appropriate thermodynamic methods and estimation of essential property parameters for simulating polyolefin processes produced by free radical polymerization. Section 4.4 presents a hands-on workshop for simulating an autoclave high-pressure (HP) LDPE process. We present an effective methodology for estimating the kinetic parameters based on plant data in the development of simulation and optimization models for commercial polyolefin processes involving free radical polymerization. Section 4.5 is another hands-on workshop for simulating tubular reactors for a high-pressure LDPE process. Section 4.6 presents a hands-on workshop for simulating an autoclave EVA copolymerization process. Section 4.7 is the bibliography.

Approximately 40% of commercial polymers are made by free radical polymerization with monomers generally in the liquid phase. Typical monomers are of the form: $XHC=CH_2$ or $XYC=CH_2$. Table 4.1 gives some examples of the monomers, repeat units, and polymers by free radical polymerization.

Table 4.1 Selected examples of free radical polymerization monomers, repeat units, and polymers

Monomer name	Monomer formula	Repeat unit	Polymer
Ethylene	$H_2C=CH_2$	$-CH_2-CH_2-$	Polyethylene(PE)
Styrene			Polystyrene (PS)
Vinyl acetate			Polyvinyl acetate (PVAC)
Ethylene-vinyl acetate (EVA)			Poly(ethylene-vinyl acetate), or EVA copolymer
Styrene and acrylonitrile			Poly(Styrene-co-acrylonitrile), or SAN copolymer
Methyl methacrylate			Poly(Methyl methacrylate) (PMMA)

4.2 Kinetics of Free Radical Polymerization

Figure 4.1 shows a schematic diagram of reactions in free radical polymerization. The key reactions include initiator decomposition, chain initiation, chain propagation, chain transfer, beta scission (spontaneous chain transfer), short-chain branching (intramolecular chain transfer or back biting), chain termination, and others as explained in the textbook by Odian [1]. In Aspen Polymers [2], a search of “Reaction Kinetic Scheme (Free-Radical)” on the online help gives a complete listing and explanations of all reactions included in the free radical polymerization model.

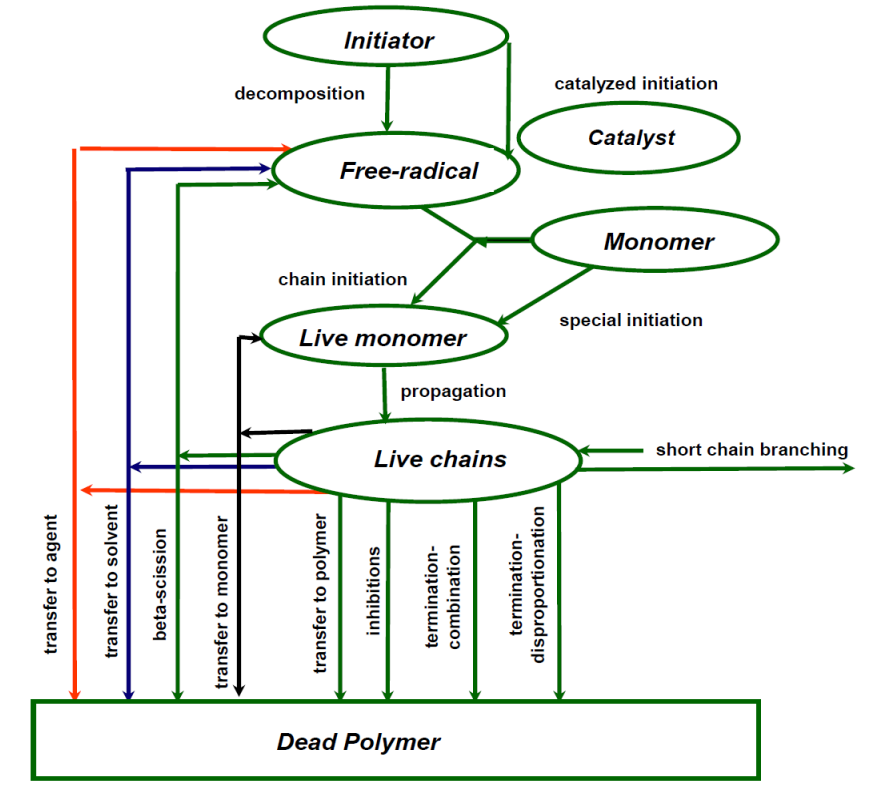


Figure 4.1 An illustration of reactions for free radical polymerization. Modified with permission. From Lingard, S., "Styrenics Modeling Seminar", Aspen Technology, Inc., Houston, TX, 2002.

4.2.1 Initiator and Its Decomposition Rate Parameters

Consider the initiator decomposition reaction: $INIT \rightarrow e \cdot n \cdot R^* + aA + bB$, where INIT represents the initiator, such as **t-butyl peroxybenzoate (TBPB)**; e is the initiator efficiency; n is the number of free radicals generated; R^* denotes the free radical; A and B are byproducts, and a and b are the corresponding stoichiometric coefficients. We use TBPB as one of our initiators in the workshop 4.1 for a high-pressure LDDE process. By searching Aspen Polymers online help for the entry of "initiator decomposition rate parameters", we can access a large collection of kinetic parameters for commercial initiators in the database, **API100 INITIATO** [3]. These initiators include azo-nitriles (both water soluble and with solvent), diacyl peroxides, peroxy carbonates, alkyl peroxides, hydroperoxides, C-C initiators, and sulfanyl peroxides. For example, Figure 4.2 shows the decomposition rate parameters for DTBP (di-tert-butyl-peroxide), which is an alkyl peroxide.

Alkyl Peroxides

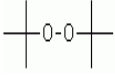
ID	Long Name	Trade Name(s)	Formula / Molecular Structure	MW	CAS No	Decomposition Rate Parameters		Decomposition Activation Energy		Half Life			Solvent	Source
						k _{ref} (1/s)	A (1/sec)	kcal/mol	GJ/kmol	1	1 hr	10 hr		
DTBP	di-tert-butyl peroxide	Trigonox B (AkzoNobel) Luperox DI (AtoFina)	C ₈ H ₁₈ O ₂ 	146.22972	110-05-4	3.7905E-09	4.36E+15	36.7	0.15346	182.9	141.0	120.7	Chlorobenzene	AkzoNobel

Figure 4.2 Decomposition rate parameters for DTBP.

Figure 4.3 shows a part of initiator decomposition reaction in the kinetic model of free radical polymerization. Within the list of free radical reactions generated by the model, we highlight the first initiator decomposition reaction, and click on “Edit Rate Constants” to access the details of the rate constant parameters. We see the specific form of the rate constant k for the initiator decomposition reaction, in which k_{ref} is the pre-exponential factor (1/sec or 1/hr), E_a is the activation energy (cal/mol or kcal/mol), ΔVP (cum/kmol or cc/mol) is the activation volume that is important in high-pressure reactions, and T_{ref} (°C) is the reference temperature. By clicking on the button “Get Rate Constants”, Aspen Polymers will fill in the relevant rate parameter values from the database **API100 INITIATO**. Note that the database assumes an initiator efficiency of 1, for which we should change to 0.8 or less in our workshop based on industrial experience. In Figure 4.3, we use an efficiency of 0.4.

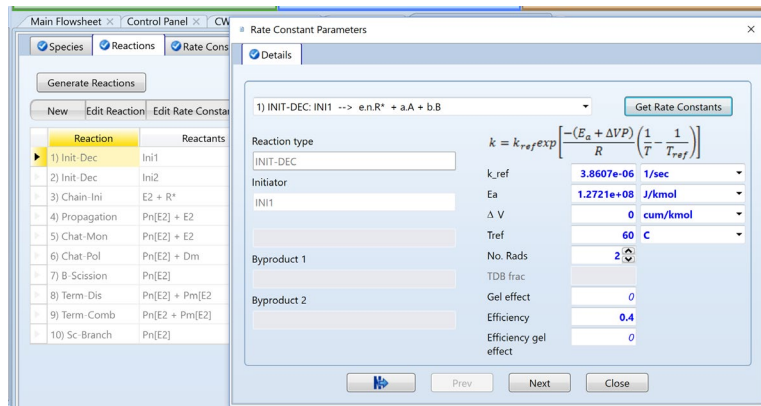
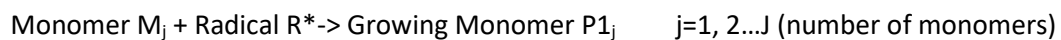


Figure 4.3 Accessing the database values of initiator decomposition rate parameters.

4.2.2 Chain Initiation Reactions

We consider three types of initiation reactions.

(1) Chain initiation (PI):



We use bracket [] to present the species concentration, and write the reaction rate as: $R_{PI,j} = k_{PI,j}[M_j][R^*]$

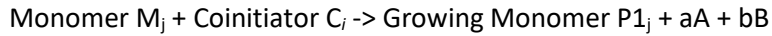
(2) Catalyzed initiation (CI):



where $i = 1, 2, \dots, I$ (number of initiators); $k = 1, 2, \dots, K$ (number of catalysts); A and B are products, and a and b are the corresponding stoichiometric coefficients.

The reaction rate of catalyzed initiation is: $R_{CI,k} = k_{CI,k}[\text{INIT}_i][\text{CAT}_k]$

(3) Special Initiation (SI):



The reaction rate of special initiation is: $R_{SI,j} = k_{SI,j} [C_i]^{a_j} [M_j]^{b_j} (h\nu)^{c_j}$

where h is Planck's constant, 6.626186×10^{-34} Joule-second; ν is the electromagnetic frequency, number of cycles per second (hertz, Hz). Depending on the values of the three exponents, this rate expression represents three cases: (i) thermal initiation, $a_j = 0, c_j = 0$; see an example of thermal initiation in the bulk solution polymerization of styrene [4]; (ii) radiation initiation, $a_j = 0$; (iii) coinitiator initiation, $c_j = 0$.

4.2.3 Chain Propagation Reactions



where $P_n(M_j)$ is a growing polymer chain of length n having an active monomer M_j segment. The rate of propagation reaction is: $R_P = k_P [M_j][P_n]$. For polystyrene, we illustrate this reaction in Figure 4.4 [5]:

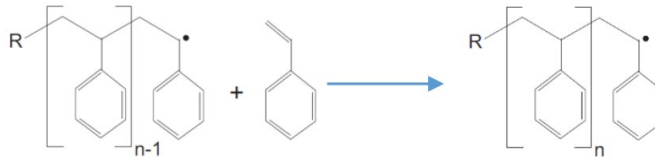


Figure 4.4 An illustration of chain propagation reaction

For copolymerization processes, such as the production of ethylene and vinyl acetate (EVA) copolymer, we need to consider the concept of *monomer reactivity ratio*. Let us consider the propagation reactions for monomers M_1 and M_2 [6]:



where $M_1 \cdot$ represents a radical of monomer M_1 . We define the reactivity ratios as follows:

$$r_1 = k_{p11}/k_{p12} \quad r_2 = k_{p22}/k_{p21}$$

We write the rates of reaction of monomers and radicals as follows:

$$-d[M_1]/dt = k_{p11} [M_1 \cdot][M_1] + k_{p21} [M_2 \cdot][M_1]$$

$$-d[M_2]/dt = k_{p22}[M_2\cdot][M_2] + k_{p12}[M_1\cdot][M_2]$$

$$d[M_1\cdot]/dt = k_{p21}[M_2\cdot][M_1] - k_{p12}[M_1\cdot][M_2]$$

$$d[M_2\cdot]/dt = k_{p12}[M_1\cdot][M_2] - k_{p21}[M_2\cdot][M_1]$$

Taking the ratio of the first two equations gives

$$d[M_1]/d[M_2] = ([M_1]/[M_2]) \{ k_{p11}[M_1\cdot]/[M_2\cdot] + k_{p21} \} / \{ k_{p22} + k_{p12}[M_1\cdot]/[M_2\cdot] \}$$

Assuming a pseudo steady-state for the radicals with $d[M_1\cdot]/dt = d[M_2\cdot]/dt = 0$, and introducing the reactivity ratios gives

$$d[M_1]/d[M_2] = ([M_1]/[M_2]) \{ r_1[M_1] + [M_2] \} / \{ [M_1] + r_2[M_2] \}$$

We see from the right-hand side of the equation that the concentration ratio of the monomers in the feed, $[M_1]/[M_2]$, and the reactivity ratios r_1 and r_2 are affecting the rate of changes of monomers in the propagation reactions. As an example, Table 4.2 shows the experimental reactivity ratios of ethylene in the radically induced polymerization with vinyl acetate at high pressures reported by Ratzsch et. al. [7].

Table 4.2 Reported reactivity ratios for EVA (ethylene-vinyl acetate) copolymerization at high pressures

Reactivity ratio $r_1 = k_{p11}/k_{p12}$	Reactivity ratio $r_2 = k_{p22}/k_{p21}$	Operating temperature (°C)	Operating Pressure	
			(atm)	(kg/cm ²)
1.2	1.1	160	1200	1240
1.2	1.1	210	1200	1240
1.2	1.1	220-240	2000	2066
1.2	1.1	220-240	2400	2480

We apply this experimental observation in our workshop WS4.3 for the EVA copolymerization.

4.2.4 Chain Transfer Reactions

We consider four types of chain transfer reactions, together with the spontaneous chain transfer reaction (beta scission) and intramolecular chain transfer (short chain branching) reaction.

(1) Chain transfer to monomer:

Growing polymer chain $P_n(M_j) + \text{Monomer } M_j \rightarrow \text{Dead chain } D_n(M_j) + \text{Growing monomer } R^*$

The reaction rate of chain transfer to monomer is: $R_{trm,j} = k_{trm,j} [P_n][M_j]$.

In this reaction, the live polymer chain (P_n) attracts a hydrogen from a monomer molecule, resulting in a dead polymer chain (D_n). The monomer, which loses a hydrogen, becomes a live polymer end group (i.e., a growing monomer) with an unreacted double bond ($P_1=$) and a free radical attaching to it. For polystyrene that we cover in Chapter 6, we illustrate the chain transfer to monomer below (the black dot represents a free radical attaching to the growing monomer) in Figure 4.5 [5]:

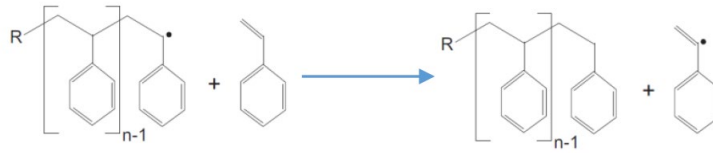


Figure 4.5 An illustration of chain transfer to monomer

(2) Chain transfer to agent:

Growing polymer chain $P_n(M_j)$ + Transfer agent $A_k \rightarrow$ Dead chain $D_n(M_j)$ + Growing monomer R^*

The reaction rate of chain transfer to monomer is: $R_{tra,k} = k_{tra,k} [P_n][A_k]$

where $k = 1, 2, \dots, K$ (number of chain transfer agents).

(3) Chain transfer to solvent:

Growing polymer chain $P_n(M_j)$ + Solvent $S_k \rightarrow$ Dead chain $D_n(M_j)$ + Growing monomer R^*

The reaction rate of chain transfer to solvent is: $R_{trs,k} = k_{trs,k} [P_n][S_k]$

where $k = 1, 2, \dots, K$ (number of solvents).

(4) Chain transfer to polymer:

Growing polymer chain $P_n(M_j)$ + Dead polymer chain $D_m(M_j) \rightarrow$ Dead polymer chain $D_n(M_j)$ + Growing polymer chain $P_m(M_j)$

The reaction rate of chain transfer to polymer is: $R_{trp,j} = k_{trp,j} [P_n][D_m]$ **(5) Spontaneous Chain Transfer or Beta Scission Reaction**

Growing polymer chain $P_n(M_j) \rightarrow$ Dead chain $D_n(M_j)$ + Growing monomer R^*

The reaction rate of beta scission is: $R_{bsc,j} = k_{bsc,j} [P_n]$

(6) Intramolecular Chain Transfer, Backbiting or Short Chain Branching Reaction:

Growing polymer chain with free radical attached to segment j , $P_n(M_j) \rightarrow$

Growing polymer with free radical attached to segment i , $P_n(M_i)$ The reaction rate of short chain branching is: $R_{scb,j} = k_{scb,j} [P_n(M_j)]$

4.2.5 Termination Reactions

(1) Termination by Combination:

Growing polymer chain, $P_m(M_j)$ + Growing polymer chain $P_n(M_j) \rightarrow$ Dead polymer chain $D(m+n)$

The reaction rate of termination by combination is: $R_{tc,j} = k_{tc,j} [P_n][P_m]$. For polystyrene, we illustrate this reaction in Figure 4.6 [5]:

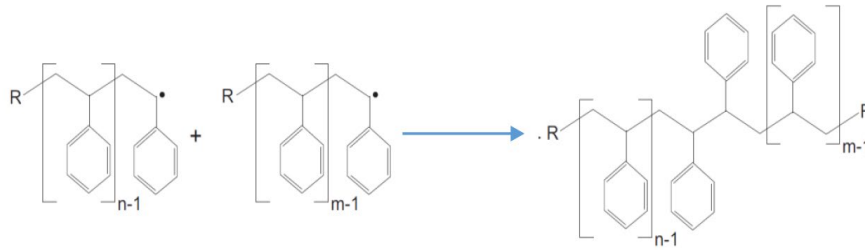


Figure 4.6 An illustration of termination by combination

(2) Termination by Disproportionation:

Growing polymer chain, $P_m(M_j)$ + Growing polymer chain $P_n(M_j)$ \rightarrow Dead polymer chain D_m + Dead polymer chain D_n

The reaction rate of termination by disproportionation is: $R_{tp,j} = k_{tp,j} [P_n][P_m]$. For polystyrene, we illustrate this reaction in Figure 4.7[5]:

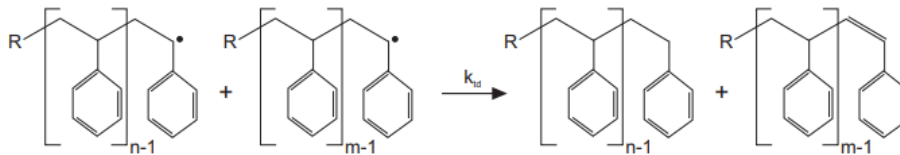


Figure 4.7 An illustration of termination by disproportionation.

4.2.6 Autoacceleration, Trommsdorff Effect, or Gel Effect

At high polymer concentrations or high conversion, termination reactions between chain radicals become diffusion-controlled, resulting in an initial increase in the polymerization rate and molecular weight. This condition is known as *autoacceleration*, *Trommsdorff effect*, or *gel effect* [1]. At high polymer concentrations, the increased viscosity of the reaction medium imposes a diffusional limitation on the polymer chains, which leads to lower effective termination rates. Typically, the termination reaction constants are affected first by the gel effect because they involve diffusion of two bulky polymer radicals. Eventually at sufficiently high conversions, even the propagation, initiation, and chain transfer reactions, and the initiator efficiency are lowered by the gel effect. Hence, in general, it may be necessary to consider gel effect for all the polymerization reactions [2].

The diffusional limitation is usually modeled by an effective reaction rate constant, k_{eff} , obtained by multiplying the low-conversion reaction rate constant, k , by a correction factor for gel effect, GF, that decreases with increasing conversion. Hence the effective reaction rate constant for a reaction is given by: $k_{eff} = k \cdot GF$.

The correction factor could be experimentally correlated with the monomer conversion [4]. We will demonstrate this correction in Workshop 6.1 for polystyrene.

4.2.7 Other Free Radical Polymerization Reactions

The Aspen Polymers model includes several other reactions: (1) head-to-head propagation, cis- and trans-propagations; (2) inhibition; (3) terminal double-bond polymerization; (4) pendent double-bond

polymerization; (5) bifunctional initiator decomposition and initiation; and (6) secondary initiator decomposition and initiation. A search of Aspen Polymers online help for the entry, “Reaction Kinetic Scheme (Free-Radical)”, gives the description of these reactions.

4.3 Thermodynamic Methods and Property Parameter Requirements

Table 4.3 summarizes several important commercial processes by free radical polymerization, the recommended thermodynamic methods for their process modeling and references for the method details, together with examples of process modeling applications.

Table 4.3 Selected polymers, thermodynamic methods, method references, and simulation examples

Polymer	Thermodynamic method	Method references	Simulation examples
Low-density polyethylene (LDPE)	POLYSL (Polymer Sanchez-Lacombe) equation of state	Section 2.6, [9-11]	[14], Workshop 4.1
LDPE	POLYPCSF (Polymer perturbed-chain statistical fluid theory) equation of state	Section 2.8, [11,16-19]	[20-24], Workshop 4.2
Poly(ethylene-vinyl acetate) (EVA copolymer)	POLYPCSF	Section 2.8, [11, 16-19, 26]	[9,28-35], Workshop 2.3
Polystyrene (PS)	POLYNRTL (Polymer non-random two-liquid) activity coefficient model	Section 2.2, [10,11]	[12], Workshop 6.1

4.4 Workshop 4.1 Simulation of an Autoclave High-Pressure LDPE Process

4.4.1 Objectives

We wish to develop a simulation model of a commercial autoclave, high-pressure LDPE process, and validate the model with plant data of production rate, MWN and MWW. We then use the validated model to do sensitivity analysis to quantify the effects of key independent variables on the polymer production rate and quality targets.

4.4.2 Process Flowsheet and Simulation Representation

Figure 4.8 shows a block flow diagram of a typical autoclave high-pressure LDPE process. The complete process consists of compression, polymerization, separation, pelleting, air conveying, mixing, processing, and package steps.

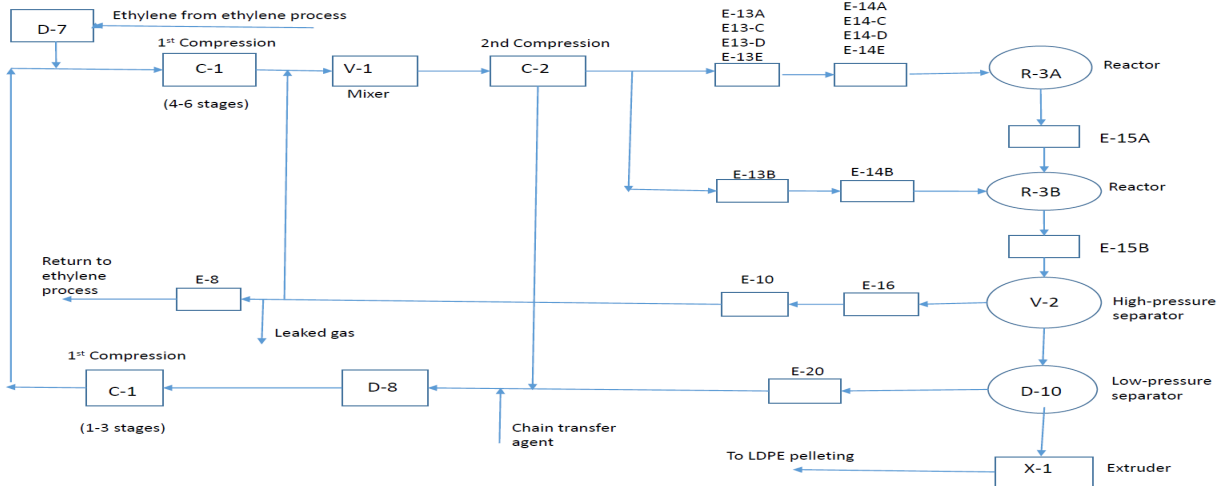


Figure 4.8 A block diagram of an autoclave high-pressure LDPE process with block numbers

In Figure 4.8, the unreacted low-pressure recycle ethylene leaving the low-pressure separator D-10 enters compressor C-1, which consists of a low-pressure section (stages 1 to 3), and a high-pressure section (stages 4 to 6). The stream leaving the low-pressure section is combined with fresh ethylene from the ethylene process in vessel D-7, and the mixed feed is further compressed in the high-pressure section. The stream leaving compressor C-1 is combined with the unreacted high-pressure recycle ethylene from the high-pressure separator V-2 in mixer V-1, followed by compression train, C21 and C22. In the figure, we see a series of exchangers before each reactor, and after the high-pressure and low-pressure separators. We draw the simulation flowsheet in three sections: (1) compression section; (2) reactor section; and (3) separation section.

Figure 4.9 shows the compression section.

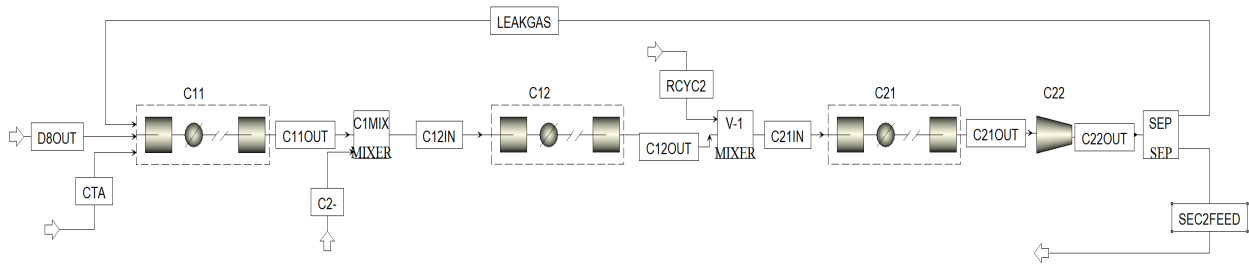


Figure 4.9. The compression section.

For the reactor section, Figure 4.10 shows a schematic diagram of two autoclave reactors in series in the LDPE process, with ethylene monomer and initiator being fed at multiple locations throughout both reactors. Reference [22] shows a similar diagram.

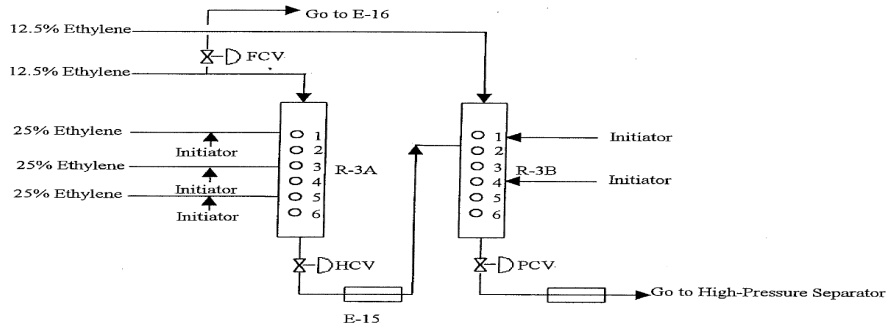


Figure 4.10 A schematic diagram of two autoclave reactors in series.

Based on Figures 4.8 and 4.10, we develop a simulation flowsheet for the reactor section. See Figure 4.11 in which continuous stirred tank reactors R3A1 to R3A3 simulate the three sections of the actual reactor R-3A, while R3B1 to R3B2 simulate the two sections of the actual reactor R-3B.

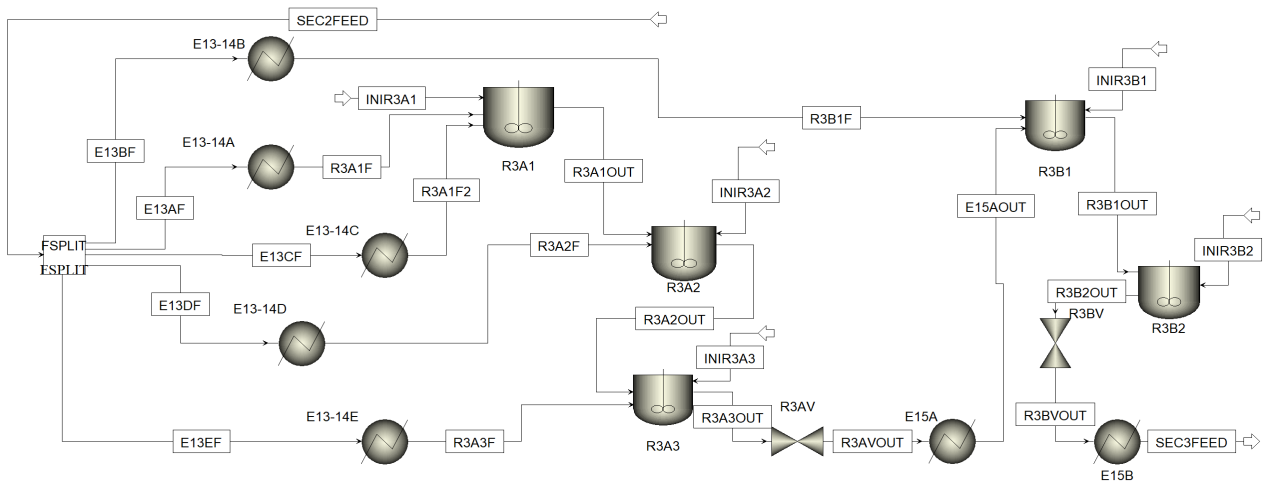


Figure 4.11 The reactor section.

After drawing both sections 1 and 2, we save the simulation as **WS 4.1 LPDE BaseCase_Secs 1-2.bkp**.

Figure 4.12 shows the separation section. We save the simulation file with all three sections as **WS 4.1 LDPE BaseCase_Secs 1-2-3.bkp**. See Figure 4.12 below.

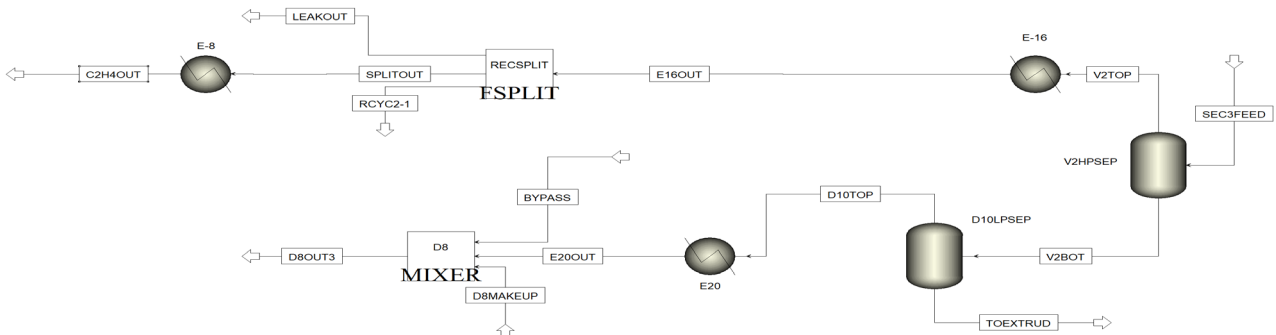


Figure 4.12 The separation section.

4.4.3 Unit System, Components and Characterization of Polymer

We define a unit system METCKGCM by copying most units from MET system, except to replace temperature unit by °C and pressure unit by kg/sqcm. See Figure 4.13.

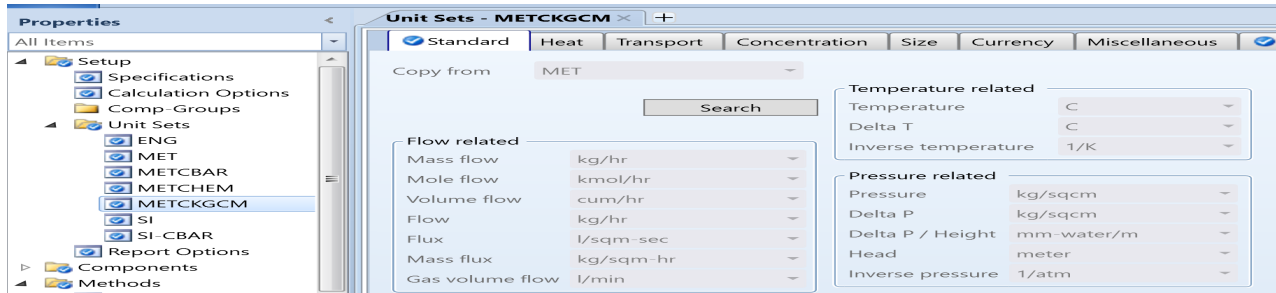


Figure 4.13 Defining a unit system METCKGCM by copying most units from MET system.

Figure 4.14 shows the enterprise databases used in the simulation of free radical polymerization processes, and Figure 4.15 specifies the components for the LDPE process.

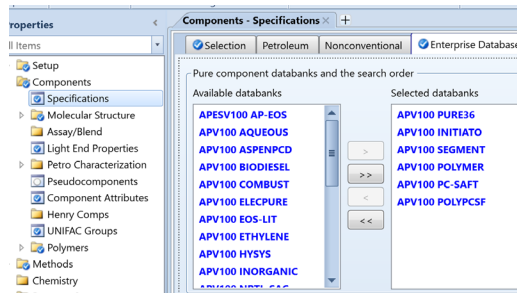


Figure 4.14 Selection of enterprise databases.

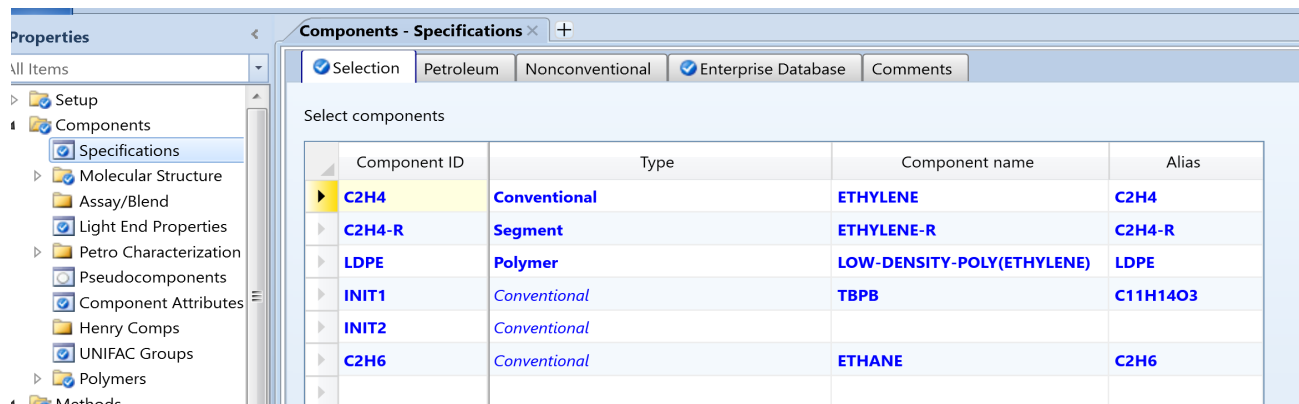


Figure 4.15 Component specifications.

C2H4 and C2H4-R are ethylene monomer, and ethylene segment (repeat type). LDPE is the polymer product. Figure 4.16 shows the definition of ethylene segment, E2-SEG or C2H4-R, and Figure 4.17 displays polymer attributes in the free radical polymerization and the attribute selection.

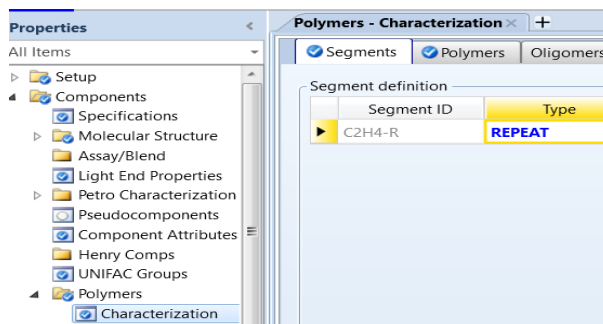


Figure 4.16 Definition of C2H4-R segment.

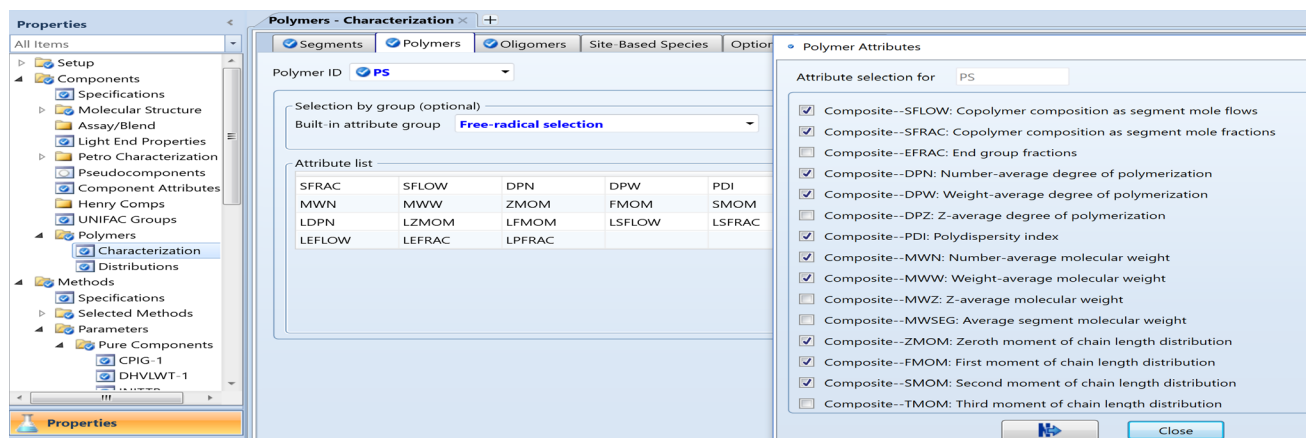
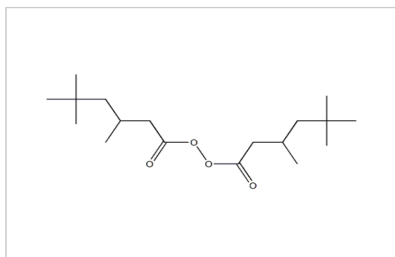


Figure 4.17 Free radical polymer attribute selection.

INIT1 is our first initiator, t-butyl peroxybenzoate, called TBPB within Aspen Polymers initiator databank, **APV100 INITIATO** (Figure 4.14), with a molecular weight of 194.23 g/mol. INIT2 is 3,5,5-trimethylhexanoyl peroxide with a chemical formula of C₁₈H₃₄O₄, a molecular weight of 314.466 g/mol and a CAS number 3851-87-4. It is *not* available within the Aspen Polymers initiator databank. To define INIT2, we search the component on the website of Chemical Book (www.chemicalbook.com). We can Google for the entry: “Chemical Book, 3,5,5-trimethylhexanoyl peroxide”, and see the structure in the first entry, as shown in Figure 4.18. We can download and save the molecular structure file, **3851-87-4.mol**, and import it into Aspen Polymers by following the path: Properties -> Components -> Molecular Structure -> INIT2 -> Structure (Graphical Structure) -> Draw/Import/Edit -> Molecule Editor -> Import Mol File -> 3851-87-4.mol -> Structure shown in Figure 4.19a.



3,5,5-Trimethylhexanoyl peroxide



3,5,5-Trimethylhexanoyl peroxide structure

CAS No.	3851-87-4
Chemical Name:	3,5,5-Trimethylhexanoyl peroxide
Synonyms	USP 355M;Peroyl 355;Trigonox 36;Dinonoyl peroxide;Initiating agent P355;Initiating agent CP-10;3,5,5-Trimethylhexanoyl peroxide;3, 5, 5-Trimethyl caproyl peroxide;Di (3,5,5-trimethylhexanoyl) peroxide;bis (3,5,5-trimethylhexanoyl) peroxide
CBNumber:	CB5855517
Molecular Formula:	C18H34O4
Formula Weight:	314.46
MOL File:	3851-87-4.mol

Figure 4.18 Search for the structure of 3,5,5-trimethylhexanoyl peroxide within Chemical Book.

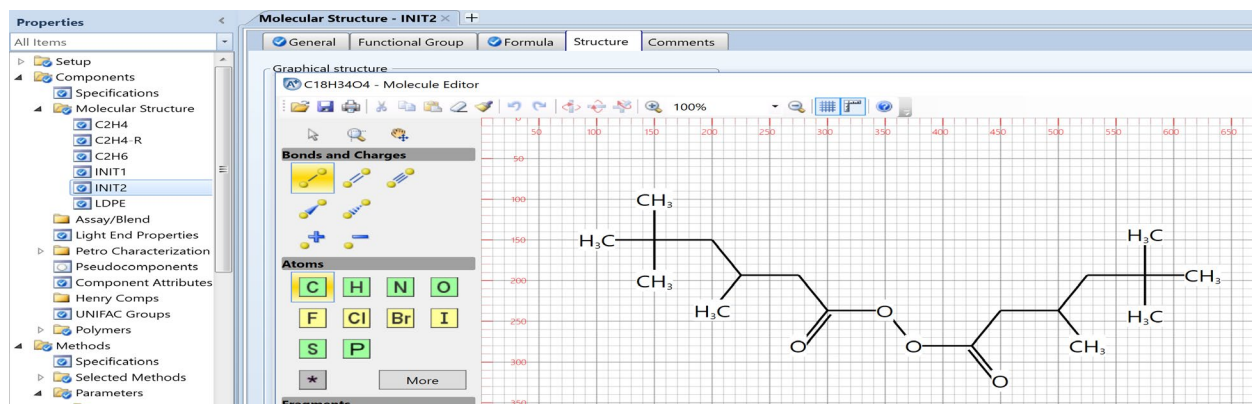


Figure 4.19a Molecular structure of INIT2 obtained by importing its MOL file from the Internet.

Next, we see the “Calculate Bonds” button, as displayed in Figure 4.19b.

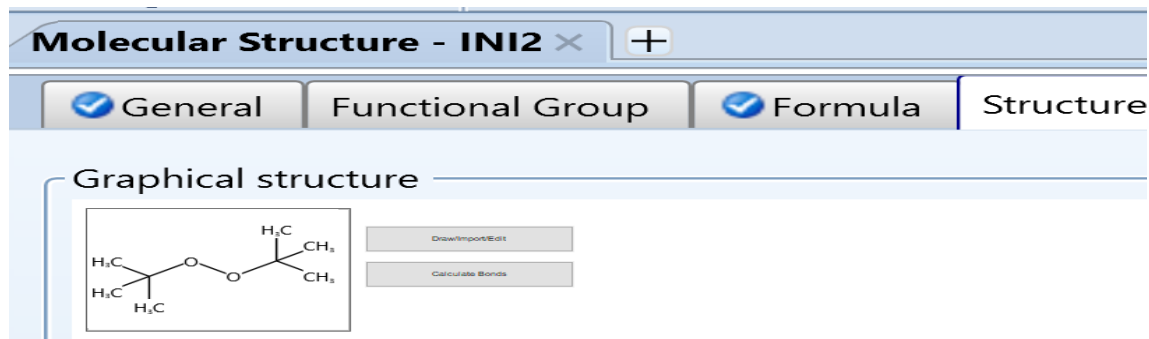


Figure 4.19b The INIT2 molecular structure and the “Calculate Bonds” button.

After clicking on the “Calculate Bonds” button, Aspen Polymers automatically completes the “General” structure folder. Figure 4.19c shows the general structure, which we will use below in the estimation of property parameters.

Atom 1		Atom 2		Bond type
Number	Type	Number	Type	
1	C	2	C	Single bond
2	C	3	C	Single bond
2	C	4	C	Single bond
2	C	5	O	Single bond
5	O	6	O	Single bond
6	O	7	C	Single bond
7	C	8	C	Single bond
7	C	9	C	Single bond
7	C	10	C	Single bond

Figure 4.19c. The molecular structure automatically defined by Aspen Polymers based on the chemical structure of Figure 9.19b.

4.4.4 Thermodynamic Methods and Property Parameters for Components, Segment and Polymer

We choose the polymer Sanchez-Lacombe (POLYSL) equation of state (see Section 2.6) for the LDPE process simulation, following an online LDPE simulation example available within Aspen Polymers [14], which also provides some essential property parameter values. We note that several references [17 to 19] demonstrate the use of perturbed-chain statistical association fluid theory (PC-SAFT) equation of state (see Section 2.8) for the LDPE process simulation, which we will illustrate in the next workshop.

Based on reference [14] and a search of Aspen Polymers help on “Sanchez-Lacombe unary parameters”, we input the pure component and segment parameters: Properties ->Methods->Parameters->Pure Components ->New -> Scalar -> Change name from Pure-1 to POLYSL -> Enter values as in Figure 4.20.

Parameters	Units	Data set	Component C2H4	Component C2H4-R	Component LDPE	Component INIT1	Component INIT2	Component C2H6
SLTSTR	K	1	333	663.15	673	530	530	315
SLPSTR	bar	1	2400	4000	3590	3040	3040	3273
SLRSTR	kg/cum	1	631	896.6	887	1120	1120	640

Figure 4.20 POLYSL pure component and segment parameters.

We enter the ideal gas heat capacity parameters for ethylene and ethylene segment in Figure 4.21 based on reference [18] by following the path: Properties-> Methods->Parameters->Pure Components ->New -> T-dependent correlation -> Ideal gas heat capacity -> CPIG-1.

Components	Source	Temperature units	Property units	1	2	3	4	5	6	7	8
C2H4	USER	K	J/kmol-K	18221.9	83.03	0	0	0	0	0	1000
C2H4-R	USER	K	J/kmol-K	33473.1	67.88	0	0	0	0	0	1000

Figure 4.21 Ideal gas heat capacity parameters

4.4.5 PCES (Physical Constant Estimation System) for Estimating Missing Property Parameters

We estimate all the missing property parameters based on molecular structures. See Figure 4.22.

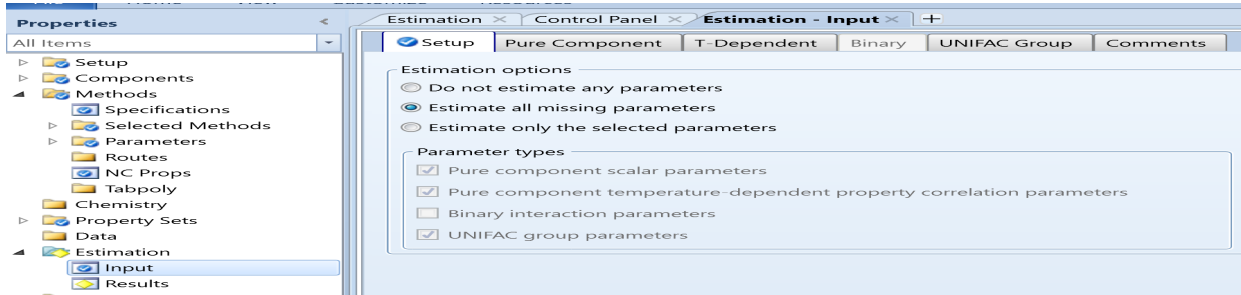


Figure 4.22 Estimation of all missing property parameters.

We then run property estimation and save the estimated parameter values before moving on to the simulation step. Figure 4.23 illustrates the estimated property values.

Parameters	Units	Data set	Component	Component	Component	Component	Component
			INIT2	C2H4-R	C2H4	C2H6	LDPE
MW		1	314.466				
TB	C	1	447.19	-27.99			
TC	C	1	634.315	128.477			
PC	kg/sqcm	1	12.277	51.291			
VC	cc/mol	1	1061.5	147.5			
ZC		1	0.169385	0.22218			
DHFORM	kcal/mol	1	-211.555	-20.1586			
DGFORM	kcal/mol	1	-124.023	-8.13031			
OMEGA		1	0.790681	0.129764			
DHVLB	kcal/mol	1	15.9017	4.7993	3.22134	3.50568	
VB	cc/mol	1	511.067	70.0472	49.3214	55.2291	
RKTZRA		1	0.216268	0.279435			0.29186
VLSTD	cc/mol	1	343.518	76.3889			298.906

Figure 4.23 An illustration of estimated property values.

4.4.6 Defining Free Radical Polymerization Reactions for LDPE

References [18,21] have described in details the relevant free radical polymerization reactions for the high-pressure LDPE process. Table 4.4 summarizes the free radical polymerization reactions for the current workshop.

Table 4.4 Free Radical Polymerizations for High-Pressure LDPE Process

Reaction	Representation	Notes
1. Initiator 1 decomposition	Initiator 1 -> Radicals INIT1 -> $\epsilon n R^* + aA + bB$ (no byproducts A and B for this initiator)	E is the decomposition efficiency, typically assumed to be 0.8. Our INIT1 or TBDP (t-butyl peroxybenzoate) generates two radicals (n=2).
2. Initiator 2 decomposition	Initiator 2 -> Radicals INIT2 -> $\epsilon n R^* + aA + bB$ (no byproducts A and B for this initiator)	Our INIT2 or 3,5,5-trimethylhexanoyl peroxide generates two radicals (n =2).
3. Chain initiation	Monomer + Radical -> Growing monomer $E2 + R^* \rightarrow P1[E2]$	$E2 = C2H4$
4. Chain propagation	Growing polymer chain + Monomer -> Propagating polymer chain $Pn[E2] + E2 \rightarrow Pn+1[E2]$	$Pn[E2]$ is a growing polymer chain of length n having an active $C2H4-R$ or $E2-R$ segment.
5. Chain transfer to monomer	Growing polymer chain + Monomer -> Dead chain + Growing monomer $Pn[E2] + E2 \rightarrow Dn + R^*$	Dn is a dead polymer chain of n segments that does not have an attached radical.
6. Chain transfer to agent	Growing polymer chain + Transfer agent -> Dead chain + Growing monomer $Pn[E2] + A \rightarrow Dn + R^*$	A represents the chain transfer agent.
7. Chain transfer to polymer	Growing polymer chain + Dead chain -> Dead chain + Growing polymer chain $Pn[E2] + Dm \rightarrow Dn + Pm+1[E2]$	
8. Beta scission (spontaneous chain transfer)	Growing polymer chain -> Dead chain + Growing monomer $Pn[E2] \rightarrow Dn + R^*$	A growing polymer chain $Pn[E2]$ breaks into a dead chain Dn and a primary radical R^*
9. Short chain branching (back biting or intramolecular chain transfer)	Growing polymer with free radical attached to segment i -> Growing polymer with free radical attached to segment j $Pn[E2] \rightarrow Pm[E2]$	
10. Chain termination by combination	Growing polymer chain Pm + Growing polymer chain Pn -> Dead polymer chain $Dm+n$ $Pn[E2] + Pm[E2] \rightarrow Dm+n$	
11. Termination by disproportionation	Growing polymer chain Pm + Growing polymer chain Pn -> Dead polymer chain Dn + Dead polymer chain Dm $Pm[E2] + Pn[E2] \rightarrow Dn + Dm$	

To generate these reactions within Aspen Polymers, follow the path: Reactions -> New: R-1 FREE-RAD type -> OK. See Figures 4.24a to 4.24b. Based on the species defined in Figure 4.24a, we click on the “generate reactions” button displayed in Figure 4.24b. Aspen Polymers automatically generates the eleven reactions in Figure 4.24b. For the reaction rate constants in Figure 4.24c, we use the pre-exponential factor and activation energy for the reaction rate constant from reference [14] as our initial values.

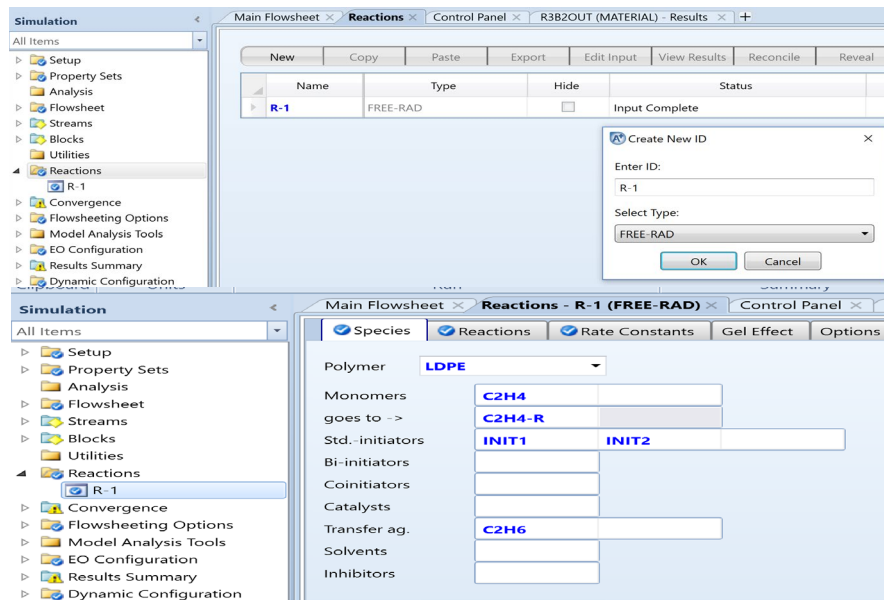


Figure 4.24a Create the free radical polymerization reaction set for LDPE process

Reaction	Reactants	Products	Active
1) Init-Dec	Init1	e.n.R* + a.A + b.B	<input checked="" type="checkbox"/>
2) Init-Dec	Init2	e.n.R* + a.A + b.B	<input checked="" type="checkbox"/>
3) Chain-Ini	C2h4 + R*	P1[C2h4]	<input checked="" type="checkbox"/>
4) Propagation	Pn[C2h4] + C2h4	Pn+1[C2h4]	<input checked="" type="checkbox"/>
5) Chat-Mon	Pn[C2h4] + C2h4	(1-f).Dn + f.Dn= + P1[C2h4]	<input checked="" type="checkbox"/>
6) Chat-Agent	Pn[C2h4] + C2h6	Dn + R*	<input checked="" type="checkbox"/>
7) Term-Dis	Pn[C2h4] + Pm[C2h4]	Dn + (1-f).Dm + f.Dm=	<input checked="" type="checkbox"/>
8) Term-Comb	Pn[C2h4] + Pm[C2h4]	Dn+m	<input checked="" type="checkbox"/>
9) Sc-Branch	Pn[C2h4]	Pn[C2h4]	<input checked="" type="checkbox"/>
10) B-Scission	Pn[C2h4]	(1-f).Dn + f.Dn= + R*	<input checked="" type="checkbox"/>
11) Chat-Pol	Pn[C2h4] + Dm	Dn Pm[C2h4]	<input checked="" type="checkbox"/>

Figure 4.24b Eleven free radical reactions for LDPE process.

Type	Comp 1	Comp 2	Pre-Exp 1/sec	Act-Energy J/kmol	Act-Volume cum/kmol	Ref. Temp. C	No. Rads [n]	TDB fraction [f]	Gel Effect	Efficiency [e]	Efficiency Gel Effect
INIT-DEC	INIT1		3.8607e-06	1.2721e+08	0	60	2		0	0.4	0
INIT-DEC	INIT2		3.7905e-09	1.5346e+08	0		2		0	0.4	0
CHAIN-INI	C2H4		2.5e+06	3.53e+07	0				0		
PROPAGATION	C2H4	C2H4	2.5e+06	3.53e+07	-0.0213				0		
CHAT-MON	C2H4	C2H4	500000	4.54e+07	0			1	0		
CHAT-AGENT	C2H4	C2H6	500000	4.54e+07	0				0		
TERM-DIS	C2H4	C2H4	5e+08	4.19e+06	0.001			1	0		
TERM-COMB	C2H4	C2H4	5e+08	4.19e+06	0.001				0		
SC-BRANCH	C2H4	C2H4	1.3e+09	4.16e+07	0				0		
B-SCISSION	C2H4	C2H4	6.07e+07	4.53e+07	0			1	0		
CHAT-POL	C2H4	C2H4	500000	3.04e+07	0.0016				0		

Figure 4.24c Initial values of kinetic parameters for LDPE process

We pause to explain how to obtain the decomposition reaction rate parameters for initiators INIT1 and INIT2 from the Aspen Polymers initiator database [3], as this will be useful to the reader when using different initiators. Specifically, we follow the path: Reactions -> Highlight reaction 1) Init-Dec, Ini1 -> Edit Rate Constants -> Rate Constant Parameters (see Figure 4.25a); change the units for pre-exponential factor k_{ref} , activation energy E_a and activation volume ΔV_P to 1/sec, J/kmol and cum/kmol, respectively -> Click on "Get Rate Constants" -> See the retrieved constants in Figure 4.25b. *Be sure to change the efficiency from a perfect value of 1 to a practical value of 0.8 or less.* We use a value of 0.4 in this workshop based on industrial experience. Repeat doing these for initiator INIT2.

Reaction type: 1) INIT-DEC: INIT1 --> e.n.R* + a.A + b.B

$$k = k_{ref} \exp \left[\frac{-(E_a + \Delta V_P)}{R} \left(\frac{1}{T} - \frac{1}{T_{ref}} \right) \right]$$

k_{ref}: 0 1/sec
 E_a: 0 J/kmol
 ΔV: 0 cum/kmol
 T_{ref}: C
 No. Rads: 2
 TDB frac: 0
 Gel effect: 0
 Efficiency: 1
 Efficiency gel effect: 0

Figure 4.25a Assessing the "rate constant parameters" screen

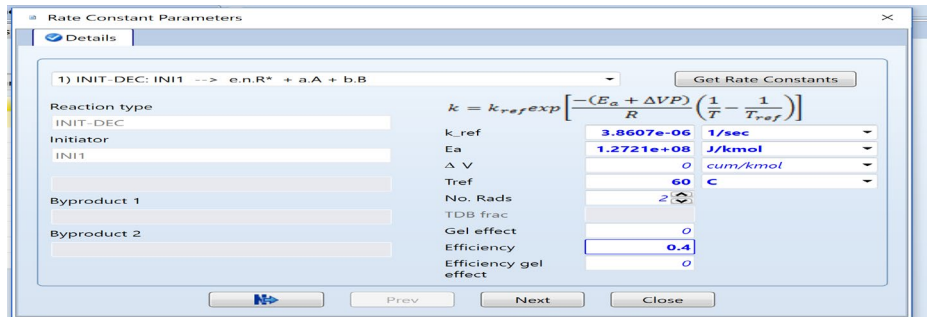


Figure 4.25b. Retrieved initiator decomposition reaction rate parameters.

4.4.7 Specifications of Inlet Process Streams and Unit Operation and Reactor Blocks

Tables 4.5 and 4.6 specify the compression and reactor sections.

Table 4.5 Specifications of the compression section.

Stream	Temperature, C	Pressure, kg/sqcm	Ethylene flow rate, kg/hr	CTA (Ethane) flow rate, kg/hr
D8OUT	40	1.433	2550	
CTA	Vapor fraction =1	4.433		40
C2-	30	34.033	9220	
RCYC2	40	251.033	25750	540
Block	Temperature, C	Pressure, kg/sqcm	Others	
C11	40 (cooler outlet)	34.033	3 stages, isentropic compression	
C1MIX		0 (no pressure drop)		
C12	40 (cooler outlet)	0	3 stages, isentropic compression	
V1	40 (cooler outlet)	0		
C21	90 (cooler outlet)	1101.033	1 stage, isentropic compression	
C22		1701.033	Isentropic compression	
SEP			CeH4 in LEAGAS = 500 kg/hr	

Table 4.6 Specifications of the reactor section.

Stream	Temp, C	Pressure, kg/sqcm	INIT1, kg/hr	INIT2, kg/hr
INIR3A1	250	1701.033	4.018	
INIR3A2	250	1601.033	2.009	
INIR3A3	250	1601.033	4.018	
INIR3B1	250	1301.033	4.571	
INIR3B2	250	1301.033	1.959	
Unit	Temp, C	Pressure, kg/sqcm	Volume, L	Reaction Set
E13-14A	35	-100		
E13-14B	35	-400		
E13-14C	35	-100		
E13-14D	35	-100		
E13-14E	35	-100		
R3A1	250	1601.033	216.67	R1
R3A2	250	1601.033	216.67	R1
R3A3	250	1601.033	216.67	R1
R3AV		1301.033		
E15A	160	0(no pressure drop)		
R3B1	240	1301.033	325	R1
R3B2	260	1301.033	325	R1
R3BV		251.033		
E15B	240	0(no pressure drop)		

We proceed to simulate the compression and reactor sections and fine-tune the reaction kinetic parameters to match the plant data before simulating the section separation.

4.4.8 Methodology for Improving Simulation Convergence and for Kinetic Parameter Estimation

Based on references [18, 21] and our industrial project experience, we propose the methodology for kinetic parameter estimation illustrated in Figure 4.26, which is particularly effective in matching polymer production targets. For polyolefin reactors operating in a small temperature range, we only estimate the pre-exponential factor k_0 and keep the activation energy E constant with values from the literature.

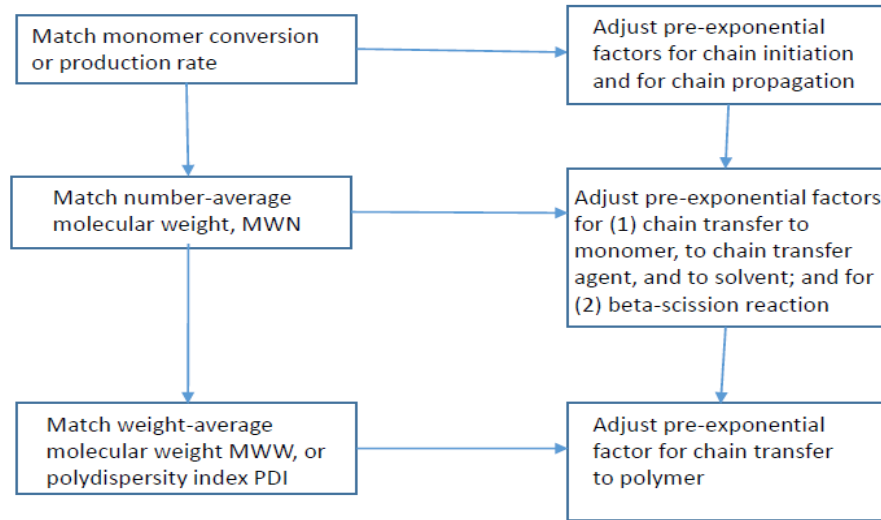


Figure 4.26 Methodology for Kinetic Parameter Estimation for LDPE Process

In adjusting the pre-exponential factors, we note the following kinetic relationship for degree of polymerization (DPN) for free radical polymerization [1]:

$$1/\text{MWN} \propto 1/\text{DPN} = k_{tr,m}/k_p + (k_{tr,A} * \text{CA}) / (k_p * \text{Cm}) \quad (4.1)$$

where the subscripts p , tr,m , and tr,A represent propagation, chain transfer to monomer, and chain transfer to chain transfer agent, respectively; CA and Cm represent the concentration of chain transfer agent and monomer, respectively. Eq. (4.1) suggests that: (1) as the pre-exponential factors for chain initiation and for chain propagation increase, the production rate or monomer conversion increases; (2) as the pre-exponential factors for chain transfer to monomer, to chain transfer agent or to solvent, and for beta-scission reaction increase, MWN decreases; and (3) as the pre-exponential factor for chain transfer to polymer increases, MWW (or PDI) increases. As we increase or decrease a specific pre-exponential factor, it is important that we do this *gradually with a small increment* for the change in the pre-exponential factor to correctly approach the simulation targets.

Our goal for simulating the base case is to quantify the kinetic parameters to match the following production targets: **(1) LPDE production rate = 8,500 kg/hr; (2) MWN = 10,500; and (3) MWW = 191,800.**

In simulating both the compression and reactor sections, we may encounter convergence issues for a recycle or tear stream, LEAKGAS in Figure 4.9, and for the five reactors in Figure 4.11. To improve the tear stream convergence, a search of “tear stream convergence” on Aspen Polymers online help gives the following recommendations on convergence parameters: (1) for Wegstein convergence scheme, increase the maximum number of flowsheet evaluations to 3000, increase the value of “Wait” to 4, increase the consecutive acceleration steps to 20, and increase the upper bound of acceleration parameter to 0.5; or (2) for the Broyden convergence scheme, increase the maximum number of flowsheet evaluations to 3000 and increase the value of “Wait” to 4 (see Figure 4.27).

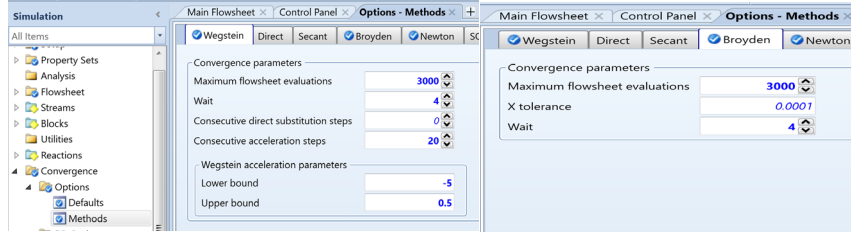


Figure 4.27 Parameter values to improve tear stream convergence.

For mass balance failure in reactor simulation, a search of “RCSTR mass balance convergence failure” on Aspen Polymers help gives the following recommendations (see also Section 3.6.5): (1) use Broyden convergence scheme, increase the number of iterations to 1000, and decrease the damping factor (0.5, 0.3, 0.1, ..., 0.0001) until the problem converges; or (2) use Newton convergence scheme with 1000 iterations and “initialize using integration”, and change the stabilization strategy from “Dogleg” to “Line search” (see Figures 4.28a and 4.28b).

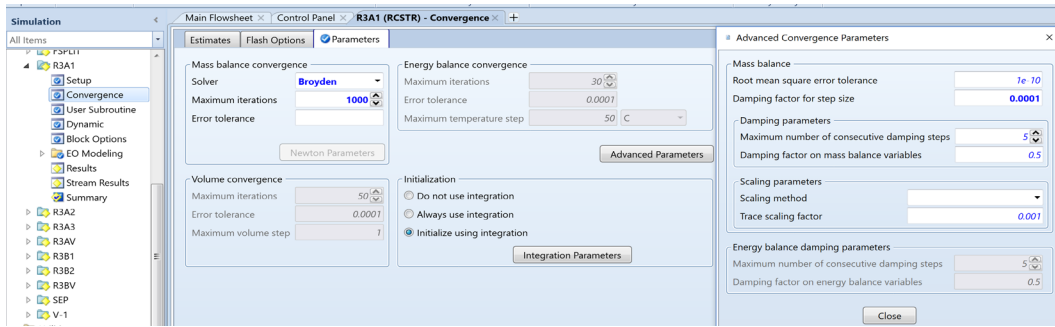


Figure 4.28a Parameter values to improve RCSTR mass balance convergence using Broyden scheme.

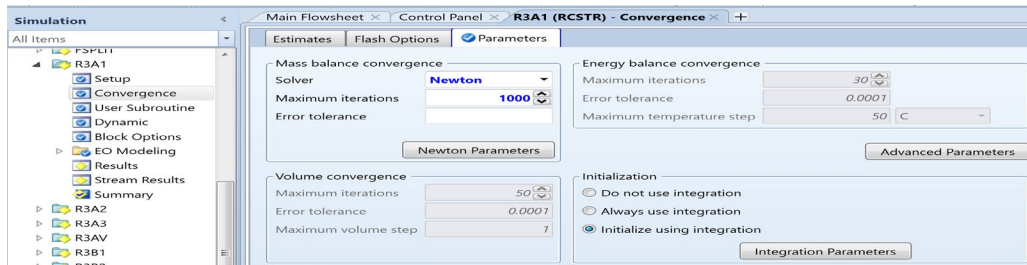


Figure 4.28b Parameter values to improve RCSTR mass balance convergence using Newton scheme.

4.4.9 Base-Case Simulation Results

Following the methodology of Figure 4.26, we fine-tune the pre-exponential factors of Figure 4.24c. Figure 4.29 shows the resulting kinetic parameters, and Figures 4.30a and 4.30b display that the simulation matches the LDPE production rate, and the corresponding MWN and MWW targets. We compare both simulation results and targets in Table 4.7. We save the resulting simulation file as ***WS4.1_LDPE_base case_good production-MWN+MWW.bkp***

Type	Comp 1	Comp 2	Pre-Exp 1/sec	Act-Energy J/kmol	Act-Volume cum/kmol	Ref. Temp. C	No. Rads	[n]	TDB fraction [f]	Gel Effect	Efficiency [e]	Efficiency Gel Effect
INIT-DEC	INIT1		4e-06	50000	0	60	2		0	0.4	0	
INIT-DEC	INIT2		4e-09	1.5346e+08	0		2		0	0.4	0	
CHAIN-INI	C2H4		2.9e+06	3.53e+07	0				0			
PROPAGATION	C2H4	C2H4	2.9e+06	3.53e+07	-0.0213				0			
CHAT-MON	C2H4	C2H4	150000	4.54e+07	0			7	0			
CHAT-AGENT	C2H4	C2H6	150000	4.54e+07	0				0			
TERM-DIS	C2H4	C2H4	5e+08	4.19e+06	0.001			7	0			
TERM-COMB	C2H4	C2H4	5e+08	4.19e+06	0.001				0			
SC-BRANCH	C2H4	C2H4	1.3e+09	4.16e+07	0				0			
B-SCISSION	C2H4		20000	4.53e+07	0			7	0			
CHAT-POL	C2H4	C2H4	34280	3.04e+07	0.0016				0			

Figure 4.29 Estimated kinetic parameters for the base case.

Material	Units	DBOUT	C2-	CTA	RCYC2	SEC2FEED	SEC3FEED
Mass Liquid Fraction		0	0	0	0	0	0.266642
Mass Solid Fraction		0	0	0	0	0	0
Molar Enthalpy	kcal/mol	12.6889	12.3234	-21.051	10.2304	12.9321	9.02723
Mass Enthalpy	kcal/kg	452.307	439.278	-700.074	364.169	460.975	321.682
Molar Entropy	cal/mol-K	-12.9185	-20.1342	-48.4194	-27.5938	-27.035	-23.8057
Mass Entropy	cal/gm-K	-0.46049	-0.717702	-1.61024	-0.98225	-0.963685	-0.848306
Molar Density	mol/cc	5.42581e-05	0.00156504	0.000259526	0.0142786	0.0186502	0.00747682
Mass Density	gm/cc	0.00152214	0.0439051	0.00780384	0.401121	0.523208	0.209819
Enthalpy Flow	Gcal/hr	1.15338	4.05014	-0.028003	9.574	17.2958	12.0748
Average MW		28.0538	28.0538	30.0696	28.0924	28.0538	28.0626
Mass Flows	kg/hr	2550	9220	40	26290	37520	37536.6
C2H4	kg/hr	2550	9220	0	25750	37520	29027.2
LDPE	kg/hr	0	0	0	0	0	8495.53
INIT1	kg/hr	0	0	0	0	0	13.8157
INIT2	kg/hr	0	0	0	0	0	0
C2H6	kg/hr	0	0	40	540	0	0

Figure 4.30a Simulated LDPE production rate of 8495.53 kg/hr.

Material	Units	DBOUT	C2-	CTA	RCYC2	SEC2FEED	SEC3FEED
- Component Attributes							
- LDPE							
DPN							387.277
DPW							6840.41
FMOM	kmol/hr						302.732
LDPN							4549.33
+ LEFLOW							
+ LEFRAC							
LFMOM	kmol/hr						0.000985001
LPFRAC							2.76983e-07
+ LSFLOW							
+ LSFRAC							
LZMOM	kmol/hr						2.16516e-07
MWN							10864.6
MWW							191899
PDI							17.6628

Figure 4.30b Simulated LDPE MWN of 10864.6, and MWW of 191899.

Table 4.7 Comparison of simulation results with production targets

	Target	Simulation	Error %
LDPE, kg/hr	8500	8495.63	0.05%
MWN	10500	10846.6	3.3%
MWW	191800	191899	0.05%

4.4.10 Model Applications

We can use the validated base-case model to do sensitivity analyses and design specification studies to identify the operating conditions to improve the current process performance. For example, while keeping the same polymer quality targets, MWN and MWW, could we increase the LDPE production rate? After conducting sensitivity analyses for varying different independent variables, we find that varying the temperatures of reactors R3B1 and R3B2 could achieve our goal.

Specifically, R3B1 temperature varies from 240 to 260 °C, while R3B2 temperature is 20 °C above the R3B1 temperature. We first define a FORTRAN (“Calculator”) block to quantify the relationship between R3B1 and R3B2 temperatures (see Figures 4.31a to 4.31c).



Figure 4.31a. Create a FORTRAN (“Calculator”) block.

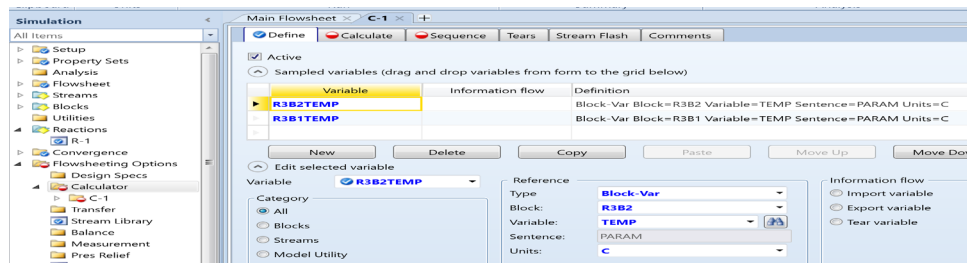


Figure 4.31b. Define the variables for the FORTRAN expression.

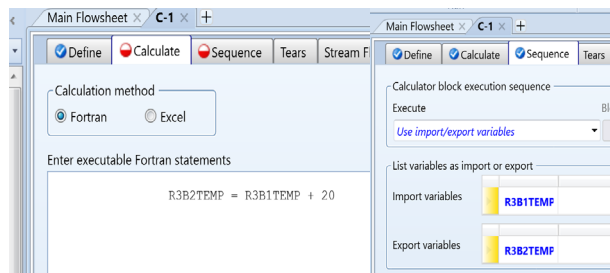


Figure 4.31c FORTRAN equation and calculation sequence.

By raising the temperature of reactor R3B1 from 240 to 260 °C and apply the Calculator to set the temperature of reactor R3B2, simulation with the validated kinetic parameters of Figure 4.29 gives the following result: **(1) LPDE production rate = 9494.43 kg/hr; (2) MWN = 10,137; and (3) MWW =198,912.** We compare these with the base-case simulation targets: **(1) LPDE production rate = 8,500 kg/hr; (2) MWN = 10,500; and (3) MWW =191,800.** This comparison suggests that we can increase the LPDE production rate by 1,000 kg/hr and obtain a MWN that is close to the target value, but with a MWW that is 7,112 above the target value. Following our methodology of Figure 4.26, we fine-tune the kinetic parameter for the pre-exponential factor for the chain transfer to polymer from 34280 to 34065, and run the simulation again, resulting in no change to the MWN, and an exact match of the MWW of 191800. We save the resulting simulation file as *WS4.1_LDPE_base case_section 2_R3B up by 20 C.bkp*.

4.4.11 Separation Section

We now add the separation section of Figure 4.12 into our simulation flowsheet (see Figure 4.32).

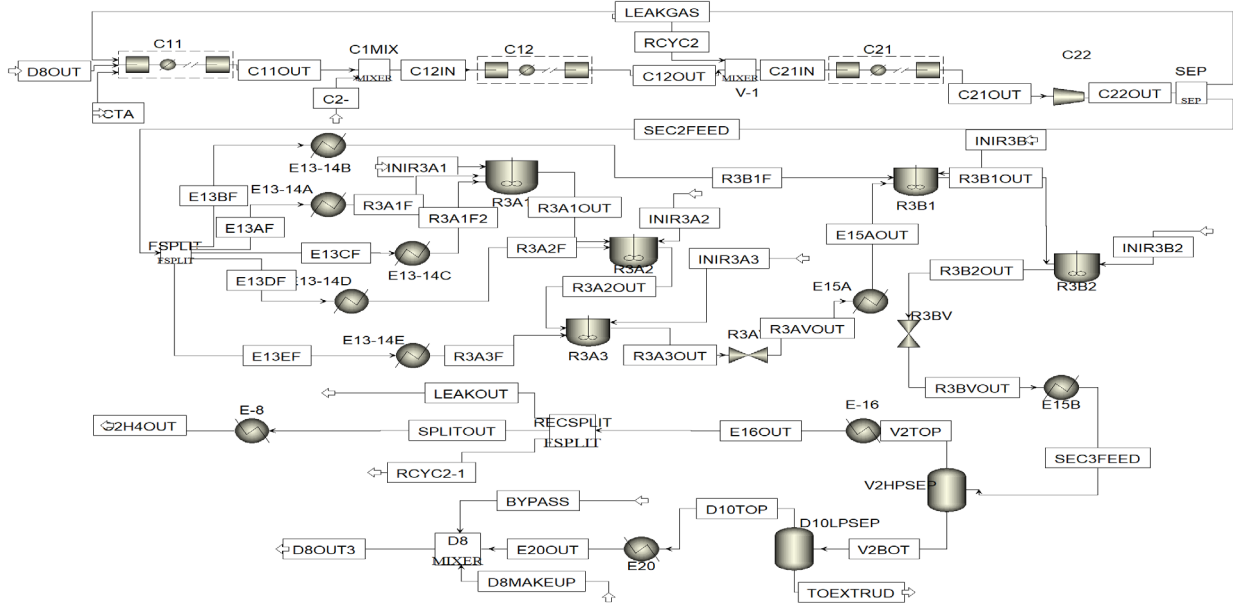


Figure 4.32 A complete flowsheet of the compression, reaction, and separation sections.

Table 4.8 shows the specifications of the separation section.

Table 4.8 Specifications of the separation section.

Stream	Temperature, C	Pressure, kg/sqcm	C2H4, kg/hr	CTA (C2H6), kg/hr
SEC3FEED				
BYPASS			0.0001	
D8MAKEUP			0.0001	
Block	Temperature, C	Pressure, kg/sqcm	Others	
V2		251.033	Vapor fraction = 0.74	
E16	40	0 (no pressure drop)		
RECSPLIT			SPLITOUT= 500 kg/hr; LEAKOUT = 260 kg/hr	
E8	120	0		
MAKEUPMX			C2H4 in HPMAKEUP = 0.0001 kg/hr	
D10	150	1.433		

Figure 4.33 shows the simulated result for our LDPE polymer product stream going to the extruder, TOEXTRUD.

Main Flowsheet		TOEXTRUD (MATERIAL) - Results (Default)				
Material	Vol.% Curves	Wt. % Curves	Petroleum	Polymers	Solids	Status
Mass Flows	kg/hr	8507.5	Component Attributes			
C2H4	kg/hr	10.8697	- LDPE			
LDPE	kg/hr	8495.53	DPN			387.277
INIT1	kg/hr	1.10517	DPW			6840.41
INIT2	kg/hr	0	FMOM	kmol/hr		302.732
C2H6	kg/hr	0	LDPN			4549.33
			+ LEFLOW			
			+ LEFRAC			
			LFMOM	kmol/hr		0.000985001
			LPFRAC			2.76983e-07
			+ LSFLOW			
			+ LSFRAC			
			LZMOM	kmol/hr		2.16516e-07
			MWN			10864.6
			MWW			191899
			PDI			17.6628
			+ SFLOW			
			+ SFRAC			
			SMOM	kmol/hr		2.07081e+06
			ZMOM	kmol/hr		0.781694
Mass Fractions						
C2H4		0.00127766				
LDPE		0.998592				
INIT1		0.000129905				
INIT2		0				
C2H6		0				

Figure 4.33 LDPE product stream going to the extruder, TOEXTRUD.

We save the resulting simulation file with all three sections as **WS4.1_LDPE_base case_Sections 1_2_3.bkp**.

4.5 Workshop 4.2. Simulation of Tubular Reactors for HP LDPE Process

4.5.1 Objectives

In addition to the stirred autoclave reactors studied in Workshop 4.1, we wish to simulate tubular reactors for making high-pressure LDPE in the current workshop. Both stirred autoclave and tubular reactors are used extensively in LDPE processes. Aspen Polymers has an example of LDPE process with tubular reactors, which uses the POLYSL equation of state (Section 2.6) for thermodynamic method, as in our last workshop. There are several articles [11,16-19] demonstrating that the POLYPCSF equation of state (Section 2.8) gives more accurate predictions for thermodynamic phase equilibrium and physical properties than the POLYSF method. In this workshop, we use the POLYPCSF thermodynamic method for our simulation. An objective of this workshop is to show how to access and estimate the required property parameters for the POLYPCSF equation of state for the simulation. Additionally, the Aspen Polymers example for the LDPE process does not deal with kinetic parameter estimation to match the simulation targets, and we wish to apply our methodology of Figure 4.26 to the current workshop. Finally, we want to show how to use an external FORTRAN subroutine for heat transfer calculations within Aspen Polymers.

4.5.2 Process Flowsheet and Simulation Representation

Figure 4.34 shows a schematic diagram of a typical high-pressure LDPE process using tubular reactors [25].

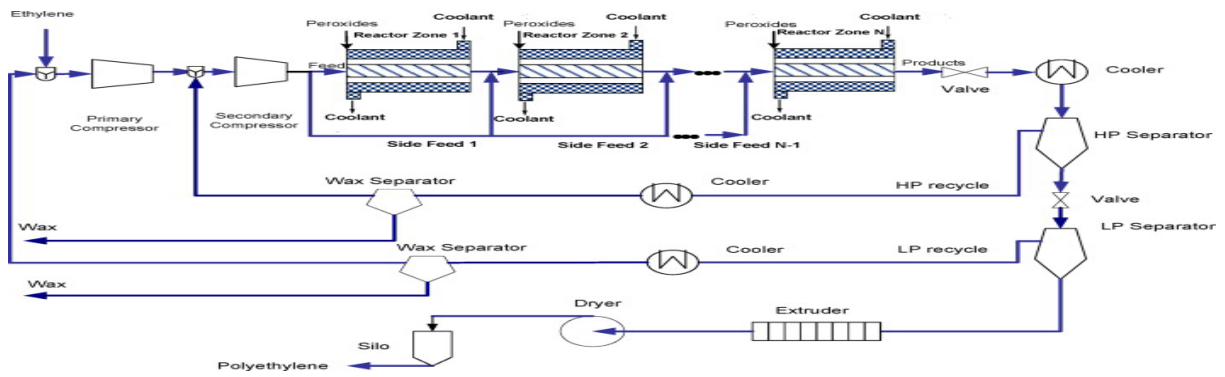


Figure 4.34 A schematic diagram of a high-pressure LDPE process using tubular reactors [25].

Following the Aspen Polymers example [14], we draw our flowsheet in Figure 4.35 to simulate most components of the process in Figure 4.34.

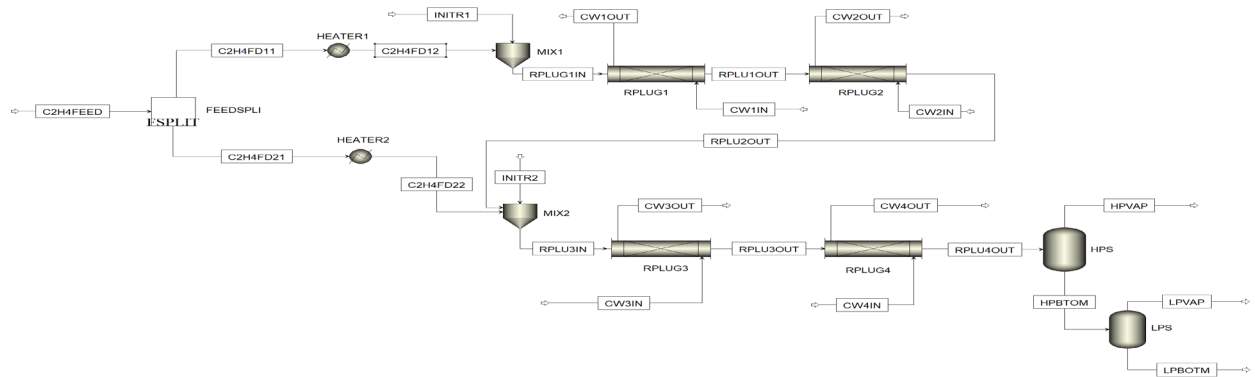


Figure 4.35 Simulation flowsheet of a tubular reactor system for high-pressure LDPE with jacketed cooling, two split feeds, four reaction zones, two initiator injection inlets modeled by four plug-flow reactors in series, plus high-pressure and low-pressure separators.

We save the simulation file as **WS4.2_LDPE BaseCase.bkp**.

4.5.3 Unit System, Components and Characterization of Polymer

We use METCBAR as our unit system. Figure 4.36 shows the component specifications.

Component ID	Type	Component name	Alias
E2	Conventional	ETHYLENE	C2H4
E2-SEG	Segment	ETHYLENE-R	C2H4-R
LDPE	Polymer	POLY(ETHYLENE)	PE
INI1	Conventional	BENZOYL-PEROXIDE	C14H10O4
INI2	Conventional	DI-T-BUTYL-PEROXIDE	C8H18O2
WATER	Conventional	WATER	H2O

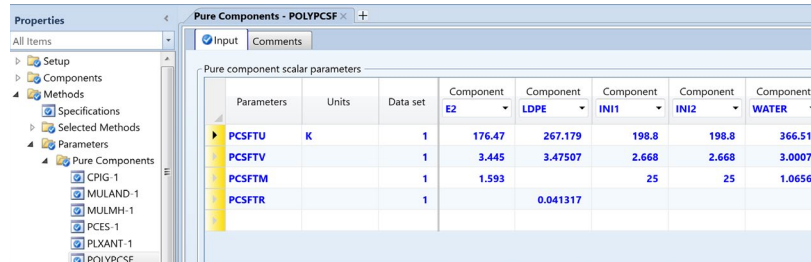
Figure 4.36. Component specifications.

We follow the procedure demonstrated previously in Figure 4.19a to 4.19c to characterize the structures of initiators INIT1 and INIT2 for use in estimating the initiator property parameters.

Following Figures 4.16 and 4.17, we define E2-SEG as a repeat segment, and choose free radical attributes for polymer LDPE.

4.5.4 Thermodynamic Method and Property Parameters for Components

We choose polymer perturbed-chain statistical fluid theory (POLYPCSF) equation of state (Section 2.8) as our thermodynamic method. Based on the original references for POLYPCSF [16,17], the Aspen Polymers LDPE example [14], and a search of Aspen Polymers online help on “Parameters (POLYPCSF)”, we input the pure component parameters: Properties -> Methods-> Parameters-> Pure Components ->New -> Scalar -> Change name from Pure-1 to POLYPCSF -> Enter values as in Figure 4.37.

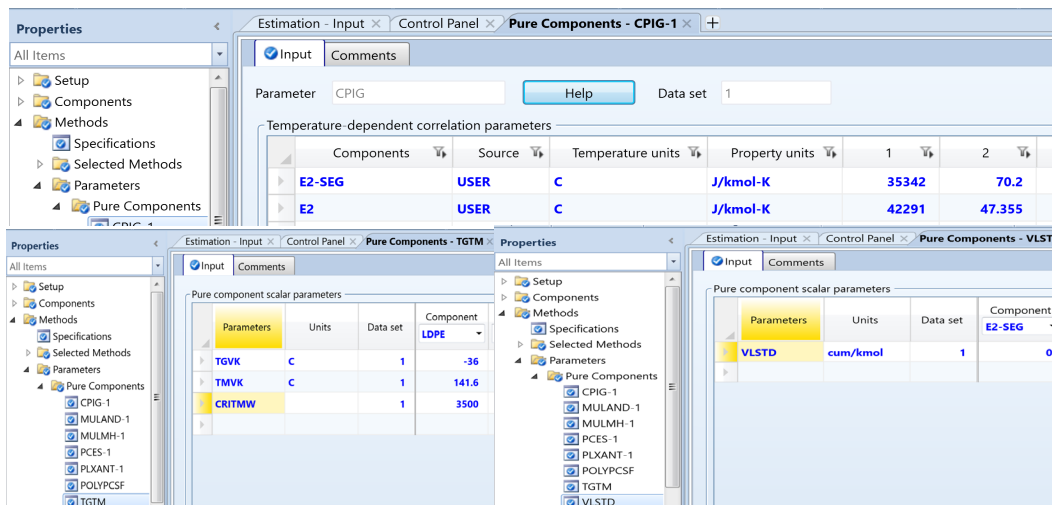


Parameters	Units	Data set	Component E2	Component LDPE	Component INI1	Component INI2	Component WATER
PCSFTU	K	1	176.47	267.179	198.8	198.8	366.51
PCSFTV		1	3.445	3.47507	2.668	2.668	3.0007
PCSFTM		1	1.593		25	25	1.0656
PCSFTR		1		0.041317			

Figure 4.37 POLYPCSF pure component parameters.

In Figure 4.37, the first three parameters are for pure components or segments. Specifically, PCSFTU is the segment energy parameter (K), PCSFTV is the segment diameter (Å), and PCSFTM is the segment number. The last parameter, PCSFTR, is a ratio parameter that is equal to PCSFTM (m) divided by the molecular weight of the monomer (M), or m/M. This parameter is reserved for polymer. When these parameters are not readily available, Aspen Polymers online help recommends the following default values: (1) $PCSFTU = 269.67 \text{ K}$, (2) $PCSFTV = 4.072 \text{ Å}$, (3) $PCSFTM = 0.02434$, and (4) $PCSFTR = 0.02434 * M$; M is the molecular weight.

Following the Aspen Polymers LDPE example [14], we enter: (1) the temperature-dependent parameters for the ideal gas heat capacity (CPIG-1) for E2 and E2-SEG; (2) the scalar van Krevelen glass transition temperature (TGVK) and melt temperature (TGVM), and polymer critical molecular weight (CRITMW) for LDPE; (3) the scalar standard liquid molar volume (VLSTD) for E2-SEG. See Figures 4.38.



Components	Source	Temperature units	Property units	1	2
E2-SEG	USER	C	J/kmol-K	35342	70.2
E2	USER	C	J/kmol-K	42291	47.355

Parameters	Units	Data set	Component LDPE
TGVK	C	1	-36
TMVK	C	1	141.6
CRITMW		1	3500

Parameters	Units	Data set	Component E2-SEG
VLSTD	cum/kmol	1	0

Figure 4.38 Pure component parameters for monomer, segment, and LDPE.

We also enter the temperature-dependent parameters for liquid vapor pressure for initiators to ensure that they do not vaporize and stay in the liquid phase: Properties-> Methods-> Parameters -> New -> T-dependent correlation -> Liquid vapor pressure -> PLXANT-1-> Enter values as in Figure 4.39. This correlation makes $\ln(\text{liquid vapor pressure of initiator}) = -40$, and makes the vapor pressure of the initiators extremely small (4.24 E-23 Bar) [8].

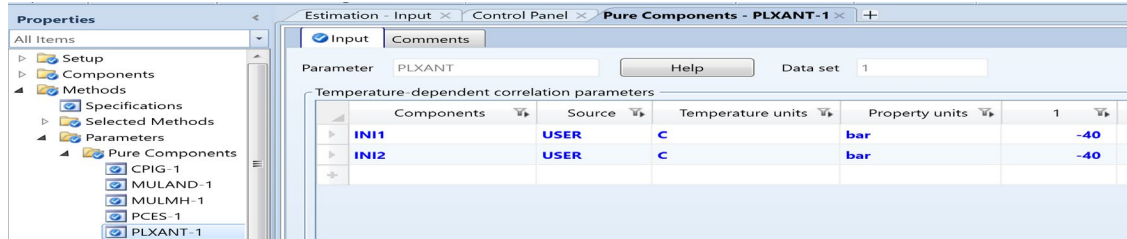


Figure 4.39 Setting the first parameter of the T-dependent liquid vapor pressure correlation PLXANT-1 to a large negative number of -40 to ensure that the initiators remain in the liquid phase.

We enter the binary interaction parameter PCSKIJ between LDPE and ethylene based on reference [17]. See Figure 4.40.

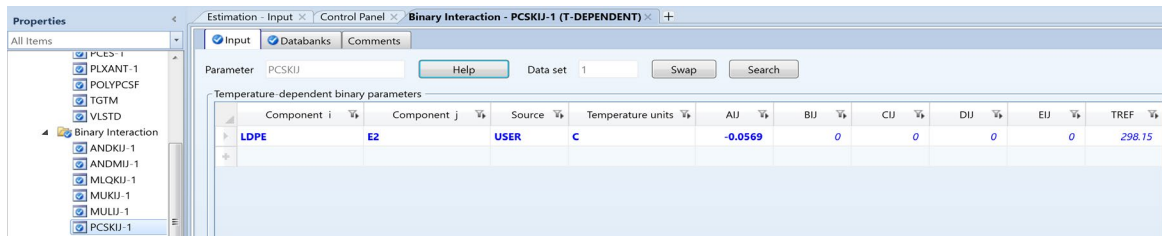


Figure 4.40 The binary interaction parameter PCSKIJ between LDPE and ethylene

4.5.4 PCES (Physical Constant Estimation System) for Estimating Missing Property Parameters

Following Figure 4.22, we estimate all missing property parameters based on molecular structures. Figure 4.41 illustrates some of the estimated property parameters.

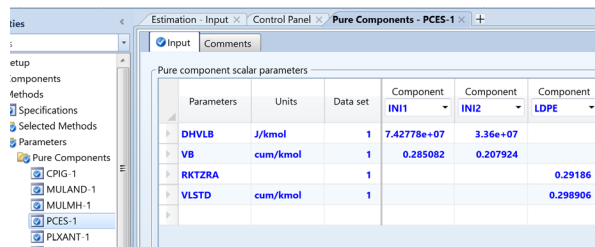


Figure 4.41 An illustration of estimated property parameters.

4.5.5 Free Radical Polymerization Reactions for LDPE

We refer the reader to the identical kinetics in Table 4.4 and Figures 4.24a to 4.24c in the previous workshop. We use essentially the same initial kinetic parameters as in the previous LDPE workshop. See Figure 4.42.

Type	Comp 1	Comp 2	Pre-Exp 1/sec	Act Energy J/kmol	Act Volume cum/kmol	Ref. Temp. C	No. Rads	(n)	TDB fraction (f)	Gel Effect	Efficiency (e)	Efficiency Gel Effect
INIT-DEC	INI1		3.8607e-06	1.2721e+08	0	60	2			0	0.4	0
INIT-DEC	INI2		3.7905e-09	1.5346e+08	0	60	2			0	0.4	0
CHAIN-INI	E2		2.5e+08	3.53e+07	0					0		
PROPAGATION	E2	E2	2.5e+08	3.53e+07	-0.0213					0		
CHAT-MON	E2	E2	1.25e+06	4.54e+07	0				1	0		
CHAT-POL	E2	E2	1.24e+06	3.04e+07	0.0016					0		
B-SCISSION	E2		6.07e+07	4.53e+07	0				1	0		
TERM-DIS	E2	E2	2.5e+09	4.19e+06	0.001				1	0		
TERM-COMB	E2	E2	2.5e+09	4.19e+06	0.001					0		
SC-BRANCH	E2	E2	1.3e+09	4.16e+07	0					0		

Figure 4.42 Initial kinetic parameter values for LDPE process

4.5.6 Specifications of Inlet Process Streams, and Unit Operation and Reactor Blocks

Table 4.9 gives the stream and block specifications.

Table 4.9 Stream and block specifications.

Stream	Temp °C	Pressure Bar	E2 kg/hr	INIT1 kg/hr	INIT2 Kg/hr	Water Kg/hr
C2H4FEED	100	2020	100000			
INITR1	0	2020		9.2	2.3	
INITR2	0	2020		18	4.6	
CW1, CW2 CW3, CW4	160	100				160000
Block	Temp, °C	Pressure, Bar	Specifications			
HEATER1	250	-10	Liquid-only			
HEATER2	250	-10	Liquid-only			
MIX1, MIX2		2000(MIX1) 1900(MIX2)	Liquid-only			
RPLUG1 RPLUG2 RPLUG3 RPLUG4	Reactor with countercurrent thermal fluid @170°; length = 250 m (RPLUG1 and RPLUG3); 200 m (RPLUG2 and RPUG4); diameter =0.059 m; pressure drop = 100 bar (process stream); 4 bar (thermal fluid); reaction set = R1					
HPS, LPS	250 bar (HPS); 1 bar (LPS)				Adiabatic, Q = 0 kcal/hr; vapor and liquid phases	

For each RPLUG reactor with external thermal fluid (cooling water), we specify in its block option the use of steam table, STEAM-TA, as the property method for the coolant stream. See Figure 4.43. We do this step for all four reactors.

Physical property methods and options		
	Process stream	Coolant stream
Property method	POLYPCSF	STEAM-TA
Henry components		
Chemistry		
Simulation approach	True components	True components
Free-water phase properties	STEAM-TA	STEAM-TA
Water solubility method	3 - No correction	3 - No correction

Figure 4.43 Specification of STEAM-TA property method for coolant stream

4.5.7 User FORTRAN Subroutine for Heat Transfer Calculations for the LDPE Reactor

The Aspen Polymers example for the LDPE tubular reactor uses a FORTRAN user subroutine, named **usrfpe.f**, to do heat transfer calculations. The reader can see the details of this FORTRAN subroutine by opening the file with a NOTEPAD, and find that the subroutine is based on heat transfer correlations reported in references [15,20]. The subroutine includes a correlation for estimating the fouling resistance, named FR, across the reactor wall, which has a unit of cm²-K-sec/cal:

$$FR = A + B*W_POL = REALQ(1) + REALQ(2)* W_POL \quad (4.2)$$

where A and B are empirical correlation parameters, corresponding to the FORTRAN code parameters, REALQ (1) and REALQ(2), with a unit of cm²-K-sec/cal; W_Pol is the weight fraction of polymer, dimensionless.

To use the subroutine, we must put the simulation file, **WS4.2_LDPE BaseCase.bkp.**, in the same working folder as the FORTRAN subroutine, **usrfpe.f**. See Figure 4.44, in which we see the values of two parameters of the fouling correlation, REALQ(1) and REALQ(2), being set to 40 and 100 cm²-K-sec/cal.

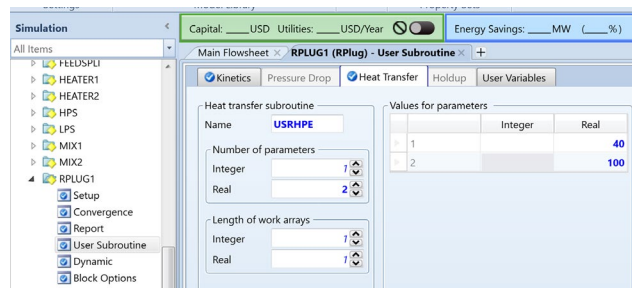


Figure 4.44. Two real parameters for the fouling correlation, REALQ(1) and REALQ(2), equal to 40 and 100 cm²-K-sec/cal.

We need to repeat the parameter specification of Figure 4.44 for all four reactors, RPLUG1 to RPLUG4.

As many readers do not have the required version of FORTRAN compiler to run the subroutine, it is helpful to convert the FORTRAN file to the corresponding dll (dynamic link library) file, and dlopt (dynamic link options) file. Fortunately, the required **userfort.dll** and **userfort.dlopt** files for heat transfer calculations are already present in the same working folder for the Aspen Polymers online LDPE example for our use without the need to compile the FORTRAN subroutine again.

The reader can check if you have the appropriate FORTRAN compiler for Aspen Polymers by checking through the path: Start->Aspen Plus->Set Compiler V10 (or higher version). If a compiler is present, you can follow the instructions on “How to compile and run an external user subroutine in an Aspen Plus simulation” (article ID 000094619, dated April 27, 2020) that is available through a search on the AspenTech support website.

To use the **userfort.dll** and **userfort.dlopt** files, we follow the path: Customize ->Options -> Run Settings -> Engine Files ->Linker Options -> “**userfort.dlopt**” (see Figure 4.45). We must give a word of caution to the reader that if you click on the dotted box to the right of the “Linker options” to search for the ***.dlopt** file, and find the file location as shown in Figure 4.46, the simulation would not work.

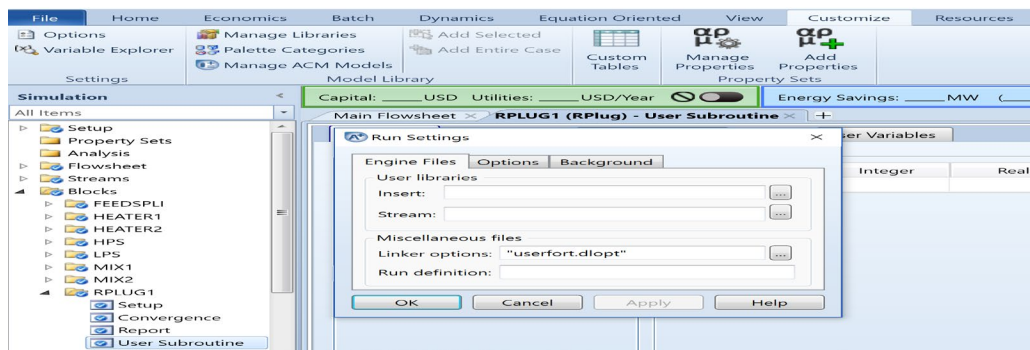


Figure 4.45 Specifying the linker options for user FORTRAN subroutine, telling the linker to use the dll file specified in the file *userfort.dlopt*.

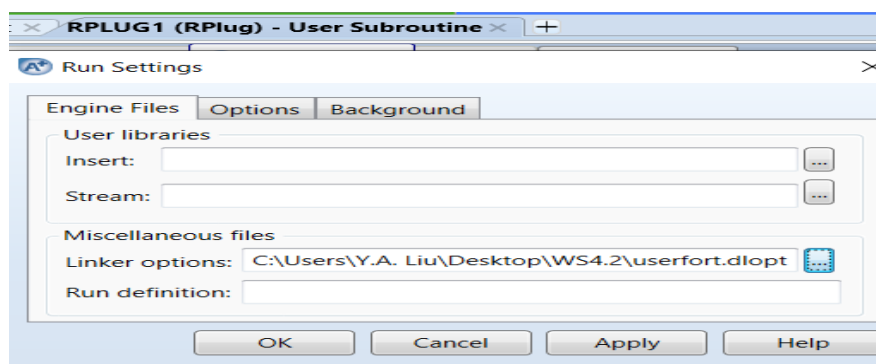


Figure 4.46 A warning: Do not link the **.dlopt* file with the detailed location on your computer drive. The simulation would not work.

4.5.8 Base-Case Simulation Targets and Kinetic Parameter Estimation

We use the same initial kinetic parameters for our LDPE process with tubular reactors as those with stirred autoclaves. See Figure 4.24c.

Our goal or simulating the base case is to identify the kinetic parameters to match the following production targets: **(1) LDPE production rate = 18,500 kg/hr; (2) MWN = 65,000; and (3) MWW = 289,000.**

Following the step-by-step procedure described in Section 4.4.8 and depicted in Figure 4.26, we fine-tune the kinetic parameters. First, by increasing the pre-exponential factors for both the chain initiation and chain propagation reactions from $2.5E8$ to $6.075E8$ 1/sec, we are able to achieve a LDPE production rate of 18,499.1 kg/hr, with a MWN of 61,245.5 and a MWW of 344,295.

Next, we decrease the pre-exponential factors for both chain transfer to monomer from $1.25E6$ to $1.075E6$ 1/sec and for beta scission from $6.07E7$ to $5.8E7$ 1/sec, resulting in a LDPE production of 18,498.7 kg/hr, a MWN of 64,192.3, and a MWW of 380,373.

To decrease MWW to 289,000, we decrease the pre-exponential factor for chain transfer to polymer from $1.24E6$ to $0.918E6$, leading to a **LDPE production of 18,487 kg/hr, a MWN of 64,202, and a MWW of 288,860**, which are very close to production targets. Figure 4.47 shows the resulting values of kinetic parameters.

Type	Comp 1	Comp 2	Pre-Exp	Act-Energy	Act-Volume	Ref. Temp.	No. Rads	[n]	TDB fraction [f]	Gel Effect	Efficiency [e]	Efficiency Gel Effect
			1/sec	J/kmol	cum/kmol	C						
INIT-DEC	INI1		3.8607e-06	1.2721e+08	0	60	2			0	0.4	0
INIT-DEC	INI2		3.7907e-09	1.5346e+08	0	60	2			0	0.4	0
CHAIN-INI	E2		6.075e+08	3.53e+07	0					0		
PROPAGATION	E2	E2	6.075e+08	3.53e+07	-0.0213					0		
CHAT-MON	E2	E2	1.075e+06	4.54e+07	0				1	0		
CHAT-POL	E2	E2	918000	3.04e+07	0.0016					0		
B-SCISSION	E2		5.8e+07	4.53e+07	0				1	0		
TERM-DIS	E2	E2	2.5e+09	4.19e+06	0.001				1	0		
TERM-COMB	E2	E2	2.5e+09	4.19e+06	0.001					0		
SC-BRANCH	E2	E2	1.3e+09	4.16e+07	0					0		

Figure 4.47 Kinetic parameter values to reach a LDPE production of 18,487 kg/hr, a MWN of 64202 and a MWW of 288,860.

We save the validated simulation file as **WS4.2_Base Case.bkp**.

We illustrate further results from this workshop. Figures 4.48a to Figure 4.48c show the “Profiles” results and how to plot the temperature profile along the length of reactor RPLUG1.

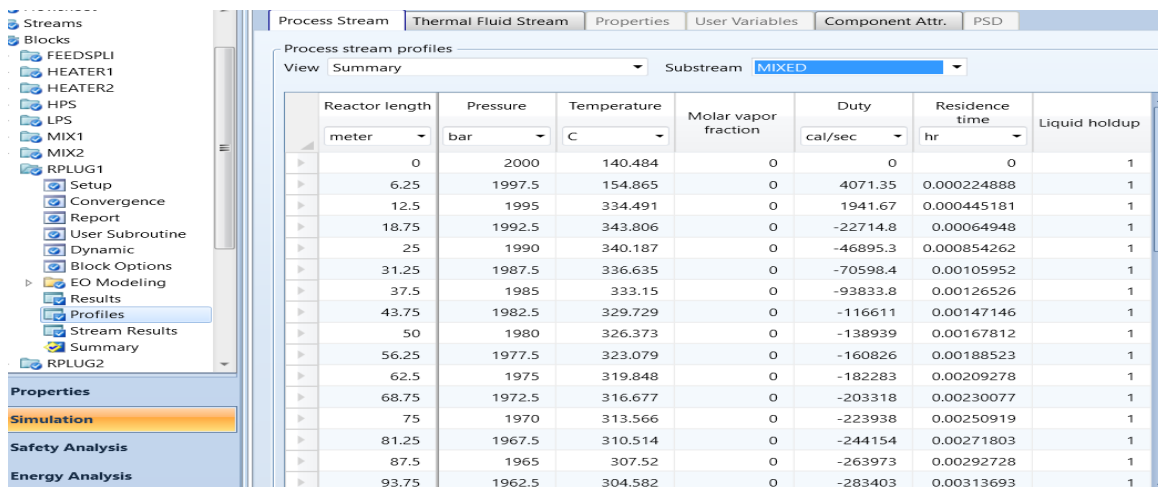


Figure 4.48a “Profiles” results from reactor RPLUG1.

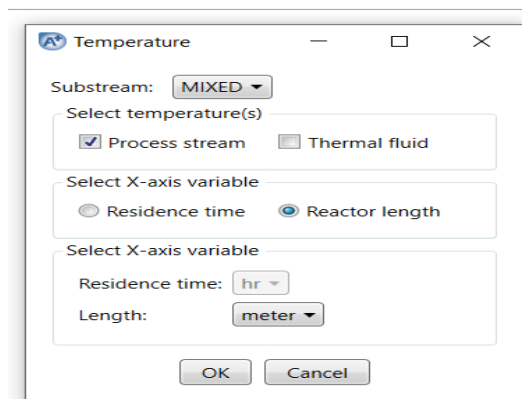


Figure 4.48b Setting up the temperature profile plot.

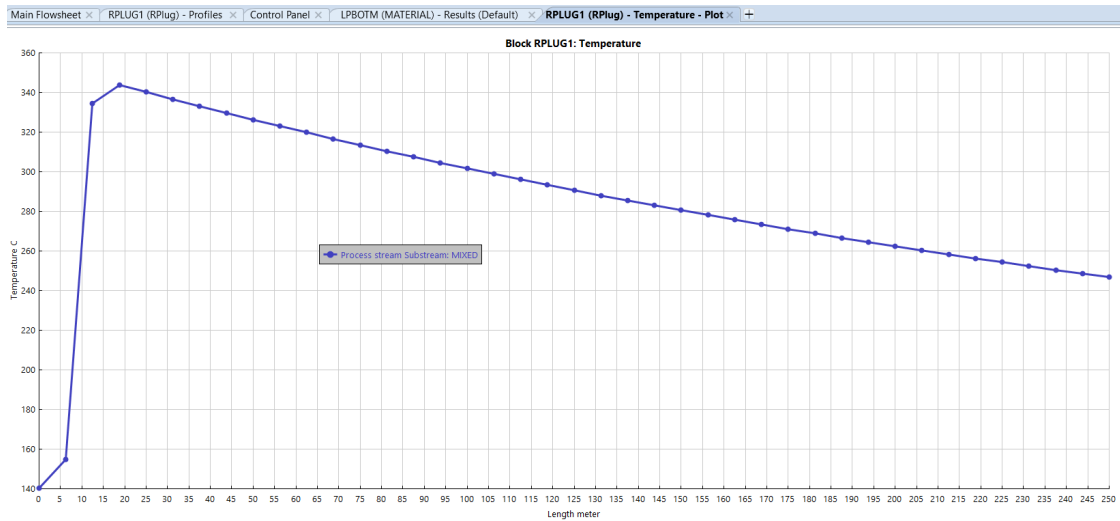


Figure 4.48c Temperature profile along the length of reactor RPLUG1

4.5.9 Model Applications

In the current flowsheet of Figure 4.35, 60% of the feed mass flow goes to the lower reactor train through the split feed, C2H4FD21. We want to investigate how does the feed split fraction affect the resulting LDPE production and the polymer MW and MWW. Figures 4.49a to 4.49c show the inputs and tabulated results of our sensitivity analysis, and Figures 4.50a to 4.50b illustrate the results graphically.

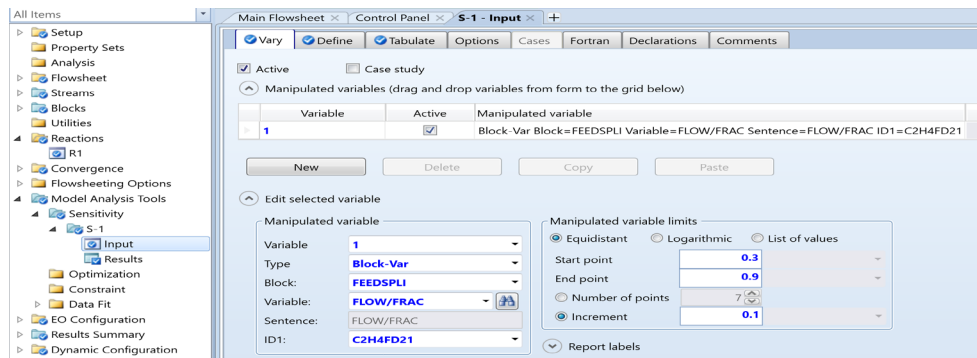


Figure 4.49a Defining the feed split fraction as the independent variable, "Vary".

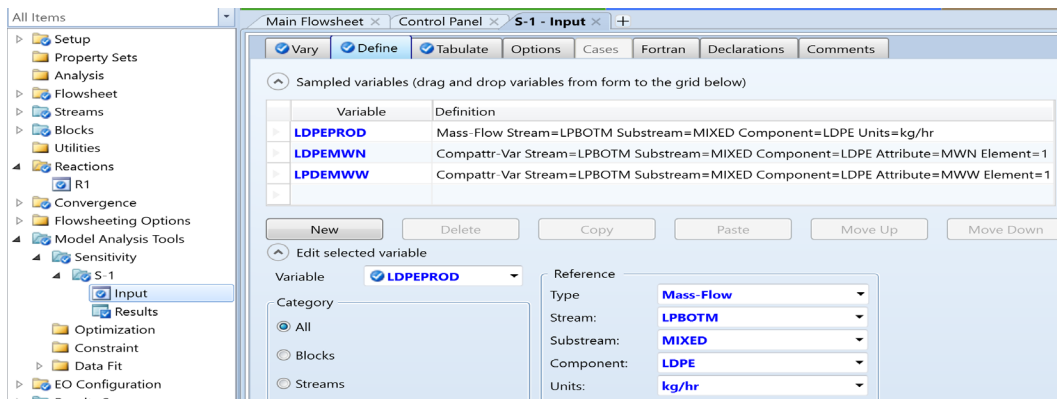


Figure 4.49b Defining the LDPR production rate, MWN, MWW as the dependent variables.

Row/Case	Status	VARY 1 FEEDSPLI C2H4FD21 FRAC FRAC	LPDEPROD KG/HR	LPDEMWN	LPDEMWW
1	OK	0.3	18590.9	61910.1	264335
2	OK	0.4	18839.1	63200.6	271968
3	OK	0.5	18901.5	64271.4	283277
4	OK	0.6	18487	64202	288860
5	OK	0.7	17514	62571.4	277107
6	OK	0.8	16296.9	60374	257562
7	OK	0.9	14994	58074	245041

Figure 4.49c Tabulating the sensitivity analysis results.

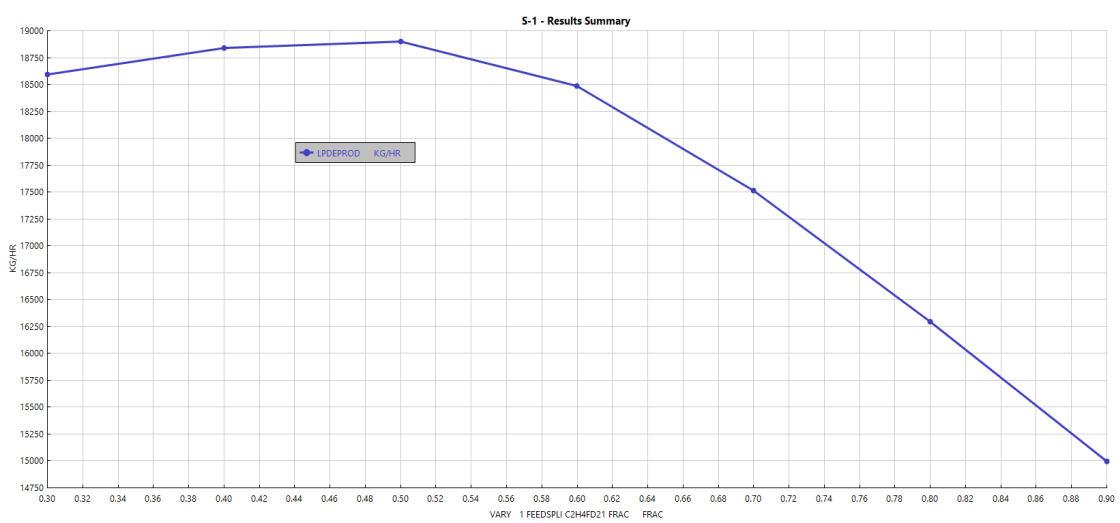


Figure 4.50a The LPDE production rate reaching a maximum at a feed split ratio of 0.5.

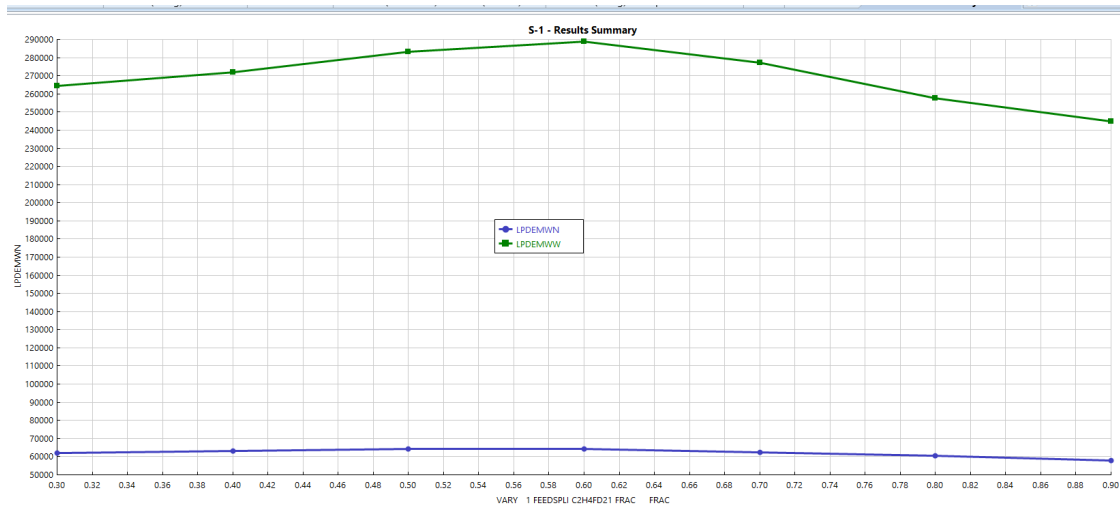


Figure 4.50b Effect of feed split ration on the polymer product MWN and MWW.

This concludes the current workshop. We save the simulation file as **WS4.2 LPDE Applications.bkp**.

4.6 Workshop 4.3 Simulation of Tubular Reactors for Ethylene-Vinyl Acetate (EVA) Copolymerization Process

4.6.1 Objective:

The objective of this workshop is to demonstrate that the methodology for simulating high-pressure LPDE process using stirred autoclave reactors or tubular reactors presented in Workshops 4.1 and 4.2 is readily applicable to simulating the EVA copolymerization process using similar reactors. While there are a number of student theses and published reports on simulating the EVA copolymerization processes [6,26-35], we can only find partial process information (such as temperature, pressure, mass flow rate of feed and product streams, chemical names of initiators, solvents, and modifiers or chain transfer agents used, operating conditions of unit operation and reactor blocks, and copolymer production targets, etc.) that are reported in separate references. As a result, we can only make educated guesses of appropriate process conditions based on published information. Additionally, these reports lack specific details in their selection of appropriate thermodynamic methods, estimation of essential property parameters, and free radical polymerization reactions. In this workshop, we focus on how to select the appropriate thermodynamic methods, property parameters, and polymerization kinetics. We show that applying our simulation methodology gives reasonable simulated results when compared to published information. We encourage those readers who have specific design and production data for an EVA copolymerization process to make appropriate changes to the current workshop and practice the application of the simulation methodology to industrial process data.

4.6.2 Process Background

Table 4.10 compares the general features of EVA copolymer production by stirred autoclave and tubular reactors [38].

Table 4.10 A general comparison of tubular and stirred autoclave reactors for EVA copolymer production

Process	Tubular Reactors	Stirred Autoclaves
Typical mass production rate per reactor train, ton/yr	400,000 ton/yr (50 ton/hr @8000 hr/yr)	150,000 ton/yr (18.75 ton/hr @8000 hr/yr)
Reactors:		
L/D ratio	1000–40000:1	10-40:1
Monomer conversion %	25-35	10-20
Heat removal	Water cooling jacket	Cold feed, hot product
Scaling	Yes	No
Pressure, MPa	240-300	130-220
Temperature, °C	250-340	150-300
Initiators	Air, O ₂ , organic peroxides	Organic peroxides
Chain transfer agents	Propylene, propane, propionaldehyde	Isobutene, n-butane
Reactor conditions:		
Feed gas	Preheating	Cooling
Temperature range	Narrow	Broad
Pressure change, MPa	30-40	<5
High pressure relief valve, impulse change	Yes	No
Start-up	Fixed pressure, gradually raise temperature	Gradually raise both pressure and temperature

Figures 4.51a and 4.51b show two published process flowsheets for high-pressure LDPE and for EVA copolymerization using stirred autoclave reactors [35,37].

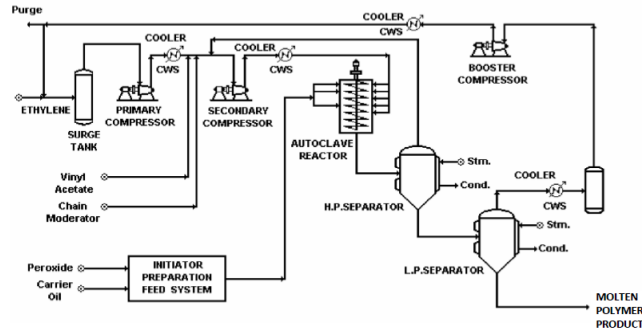


Figure 4.51a Flowsheet of the EVA copolymerization using a stirred autoclave reactor [35]

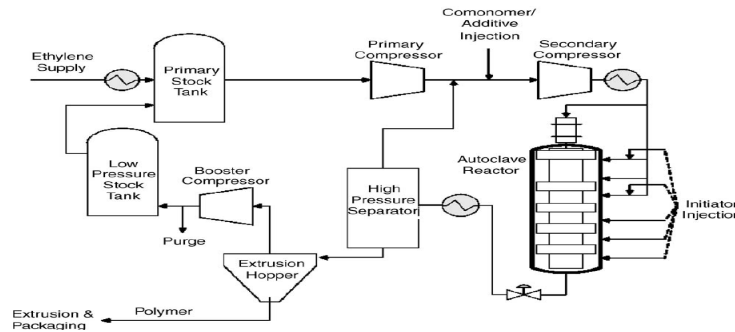


Figure 4.51b Flowsheet of the ICI high-pressure autoclave reactor technology for LDPE production and for EVA copolymerization with minor modification [37]

The autoclave reactor in Figure 4.51a has seven reaction zones, with reaction feeds entering in zones 1 to 5 zones, and the initiator feeds entering zones 1, 2 and 4. We could modify our previous stirred autoclave reactor system for LDPE production in Figures 4.10 to 4.11 to develop a simulation flowsheet for the EVA copolymerization reactor section. For example, Figure 4.52 shows the autoclave reactor section of our flowsheet.

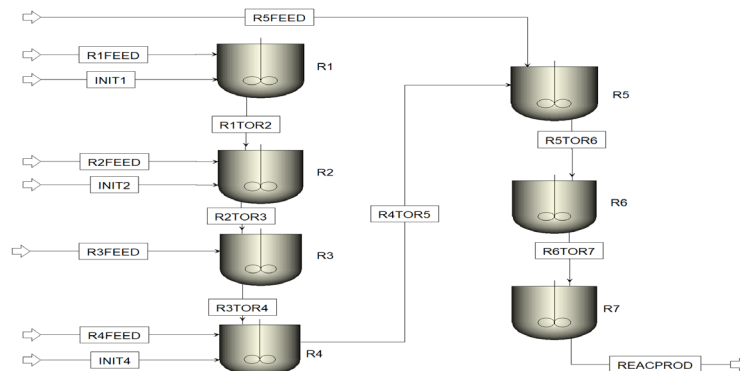


Figure 4.52 Simulation flowsheet of the stirred autoclave reactor for EVA copolymerization.

In this workshop, we focus on simulating the tubular reactor system for producing EVA copolymer. We modify our previous tubular reactor system for LDPE production in Figures 4.34 to 4.35 to develop a simulation flowsheet for the EVA copolymerization reactor section. For convenience, we modify the

simulation file, **WS4.2_LDPE Base Case** from Workshop 4.2. Figure 4.53 shows the reactor section of our flowsheet. We save the simulation file as **WS4.3.bkp**.

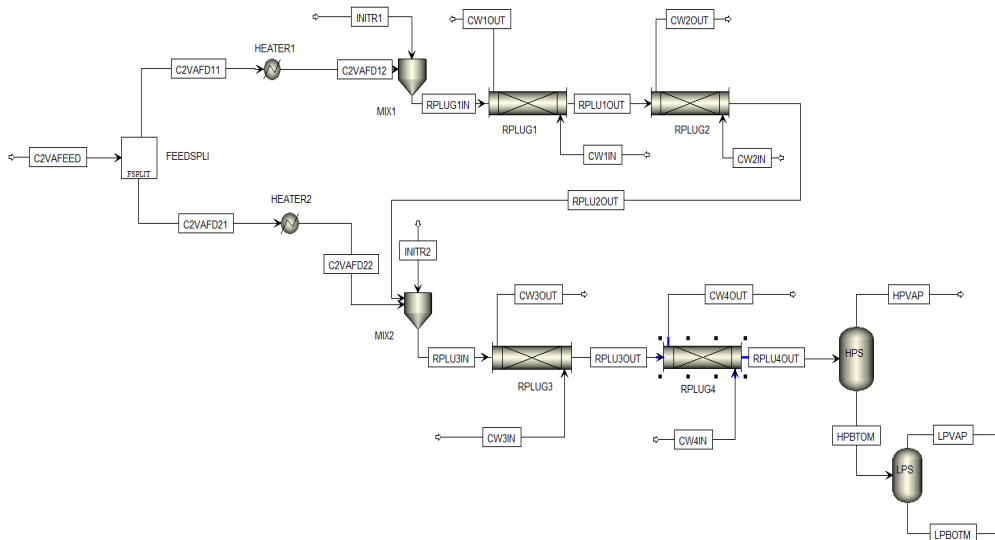


Figure 4.53 Simulation flowsheet of a tubular reactor system for high-pressure EVA copolymerization with jacketed cooling, two split feeds, four reaction zones, two initiator injection inlets modeled by four plug-flow reactors in series, plus high-pressure and low-pressure separators.

4.6.3 Unit System, Components and Characterization of Polymer

We choose METCBAR as our unit system. Figure 4.54 shows our component specifications for the EVA copolymerization process. Following reference [28], we choose TBPEH (tert-butylperoxy-2-ethylhexanoate; CAD number 3006-82-4) as our initiator. Other potential initiators are TBPND (tert-butyl peroxyneodecanoate; CAS number 26748-41-4), TBPB (t-butyl peroxybenzoate; CAS number 614-45-9); and TBPPI (t-butyl peroxy-pivalate; CAS number 927-07-1). All four are available within Aspen Polymers initiator database. For modifiers or chain transfer agents, the literature suggests propylene [28, 38] or propane [38] for tubular reactors, and isobutylene and n-butane [38] for stirred autoclave reactors; and n-hexane [27] as our solvent. Additionally, we follow Figures 4.16 and 4.17 to define our repeat segments, E2-R and VA-R, and our polymer POLYEVA, together with the selection of attributes for free radical polymerization.

Component ID	Type	Component name	Alias
E2	Conventional	ETHYLENE	C2H4
E2-R	Segment	ETHYLENE-R	C2H4-R
VA	Conventional	VINYL-ACETATE	C4H6O2-1
VA-R	Segment	VINYL-ACETATE-R	C4H6O2-R-3
POLYEVA	Polymer	POLY(ETHYLENE-VINYL-ACETA...	PE&VAC)
TBPEH	Conventional		
CTA	Conventional	PROPYLENE	C3H6-2
SOLVENT	Conventional	N-HEXANE	C6H14-1
WATER	Conventional	WATER	H2O

Figure 4.54 Component specifications

We also follow Figures 4.18 and 4.19a to 4.19c to obtain the chemical structures of initiators TBPEH and TBPND and characterize their general structures according to bond types. See the example file folder for

Chapter 4 for *TBPEH.mol* and *TBPND.mol*. Figure 4.55 illustrates the chemical structure of TBPEH obtained from the initiator database of Aspen Polymers, API100 INITIATO.

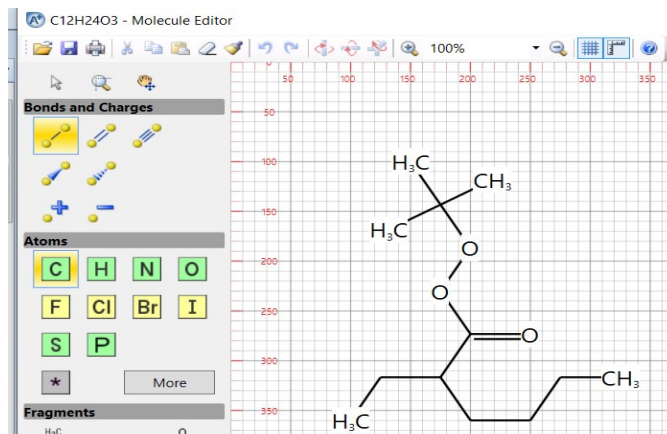


Figure 4.55 Chemical structure of initiator TBPEH.

4.6.4 Thermodynamic Method and Property Parameters for Components and Polymer

We follow Figure 4.37 in the previous workshop for high-pressure LDPE, and choose POLYPCSF as our thermodynamic method, and enter the required pure component parameters in Figure 4.56.

Parameters	Units	Data set	Component E2	Component E2-R	Component VA	Component VA-R	Component TBPEH	Component CTA	Component SOLVENT	Component WATER
PCSFTU	K	1	176.47	267.179	232.25	243.983	198.8	207.19	236.77	269.67
PCSFTV		1	3.445	3.47507	3.257	3.0617	2.668	3.5356	3.7983	4.072
PCSFTM		1	1.593		3.442		25	1.9598	3.0576	0.02434
PCSFTR		1		0.041317		0.04224				

Figure 4.56 Pure component and segment parameters.

In the figure, PCSFTU is the segment energy parameter (K), PCSFTV is the segment diameter (Å), and PCSFTM is the segment number. The last parameter, PCSFTR, is a ratio parameter that is equal to PCSFTM (m) divided by the molecular weight of the monomer (M), or m/M. This parameter is reserved for polymer. We find the parameter values for E2, VA, propylene (a chain-transfer agent, CTA), n-butane (another CTA), solvent (hexane) and water from [16, 17, 28], and for E2-R and VA-R from [26]; we assume the values for initiator TBPEH following [14]. For propylene, we follow the values given in Figure 2.53.

Following Figure 4.22, we estimate all missing parameters using molecular structure-based estimates. As an example, Figure 4.57 shows the resulting parameters for the temperature-dependent ideal-gas heat capacity correlation, CPIG-1.

Components	Source	Temperature units	Property units	1	2	3	4	5	6
E2-R	USER	C	J/kmol-K	35342	70.2				
E2	USER	C	J/kmol-K	42291	47.355				
VA-R	DB-SEGMENT	C	J/kmol-K	95373.6	302.445	-0.356588	0.000196	0	0
TBPEH	R-PCES	C	J/kmol-K	282679	902.843	-0.678471	0.000225754	0	0
VA	R-PCES	C	J/kmol-K	96901.6	241.578	-0.124804	-3.3e-06	0	0

Figure 4.57 Parameter values for temperature-dependent, ideal-gas heat capacity correlation, CPIG-1.

Following Figure 4.39, we enter a parameter value of -40 for liquid vapor pressure, PLXANT, for initiator TBPEH, to ensure that it stays in the liquid phase and does not vaporize. See Figure 4.58.

Components	Source	Temperature units	Property units	1	2	3	4	5	6
E2-R	R-PCES	C	bar	29.9741	-3263.41	0	0	-3.02832	5.37789e-17
VA-R	R-PCES	C	bar	51.0394	-5986.41	0	0	-5.79084	1.5412e-17
E2	DB-PURE36	C	bar	42.4501	-2443	0	0	-5.5643	1.9079e-05
VA	DB-PURE36	C	bar	45.8931	-5702.8	0	0	-5.0307	1.1042e-17
CTA	DB-PURE36	C	bar	32.3921	-3097.8	0	0	-3.4425	9.9989e-17
WATER	DB-PURE36	C	bar	62.1361	-7258.2	0	0	-7.3037	4.1653e-06
TBPEH	USER	C	bar	-40	0	0	0	0	0

Figure 4.58 Parameter values for temperature-dependent, Antoine vapor-pressure correlation, PLXANT

4.6.5 Free Radical Polymerization Kinetics for EVA Copolymerization

We expand the reaction set for free radical polymerization for high-pressure LDPE in Table 4.4 to include the addition of a comonomer, VA, and the corresponding changes to the chain initiation, chain propagation, chain transfer, and chain termination reactions, and to the beta scission and short chain branching reactions involving both the monomer E2 and comonomer VA. This results in Table 4.11, in which we have also added the initial kinetic parameter values based on the literature.

Table 4.11 Initial parameters for free radical polymerization kinetics for EVA copolymerization

Reaction	Comp. 1	Comp. 2	Pre-exponential Factor, 1/sec	Activation energy, cal/mol	Activation volume, Cum/kmol	References	Notes
Initiator decomposition TBPND			1.1742E-4	25759.5	0	[3,30]	Initiator efficiency = 0.4; number of radicals = 2
Initiator decomposition TDPEH			4.1442E-6	29831.9		[3,30]	Same as above
Chain Initiation*	E2		1.25E8	7550.6	-0.02	[16,30]	
	VA		1.47E7	4947.6	-0.0107	[16,30]	
Chain Propagation	E2(1)	E2(1)	1.25E8	7550.6	-0.02	[7,30,36]	
	E2(1)	VA(2)	1.148E8	7550.6	-0.02	[7,30,36]	$K_{p,11} = 1.09 * K_{p,12}$ [7]
	VA(2)	VA(2)	1.47E7	4947.6	-0.0107	[7,30,36]	
	VA(2)	E2(1)	1.387E7	4947.6	-0.0107	[7,30,36]	$K_{p,22} = 1.06 * K_{p,21}$ [7]
Chain transfer to monomer	E2(1)	E2(1)	8.7E5	9998.6	-0.02	[30]	
	E2(1)	VA(2)	8.7E5	9998.6			assumed
	VA(2)	VA(2)	7.616E3	6298.8			assumed
	VA(2)	E2(1)	7.616E3	6298.8			assumed
Chain transfer to agent	E2(1)	CTA	8.7E5	9998.6	-0.02		assumed
	VA(1)	CTA	7.163E3	6298.8			assumed
Chain transfer to polymer	E2(1)	E2(1)	4.78E8	13120.1	0.0044	[30]	
	E2(1)	VA(2)	4.78E8	13210.1	0.0044		assumed
	VA(2)	VA(2)	1.088E4	6298.8		[30]	
	VA(2)	E2(1)	1.088E4	6298.8			assumed
Termination by (1) combination and (2) disproportionation	E2(1)	E2(1)	1.25E9	649.4	0.013	[30]	
	E2(1)	VA(2)	1.25E9	649.4	0.013		assumed
	VA(2)	VA(2)	3.7E9	3199.1		[30]	
	VA(2)	E2(1)	3.7E9	3199.1			assumed
Beta scission	E2(1)		1.292E7	11268.3		[30]	
	VA(2)		1.292E7	11268.3			assumed
Short-chain branching	E2(1)		1.6E8	10942.4	0.0229	[30]	
	VA(2)		1.6E8	10942.4			assumed

*Set chain initiation rate constant equal to or larger than chain propagation rate constant [36]; assume the same termination rate constants by combination and by disproportionation.

We follow the procedure in the previous workshops to generate a reaction set R-1 based on the free radical polymerization model within Aspen Polymers for EVA copolymerization. Figures 4.59 and 4.60 illustrate the specification of species and the resulting reactions for EVA copolymerization. Refer to Table 4.11 for the values of initial kinetic parameters.

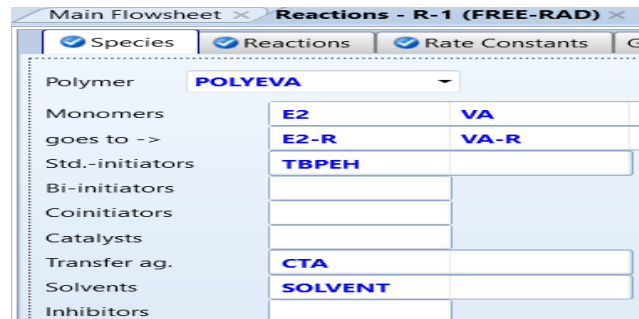


Figure 4.59 Specification of species for EVA copolymerization

Reaction	Reactants		Products
1) Init-Dec	Tbpeh	->	e.n.R* + a.A + b.B
2) Chain-Ini	E2 + R*	->	P1[E2]
3) Chain-Ini	Va + R*	->	P1[Va]
4) Propagation	Pn[E2] + E2	->	Pn+1[E2]
5) Propagation	Pn[E2] + Va	->	Pn+1[Va]
6) Propagation	Pn[Va] + E2	->	Pn+1[E2]
7) Propagation	Pn[Va] + Va	->	Pn+1[Va]
8) Chat-Mon	Pn[E2] + E2	->	(1-f).Dn + f.Dn= + P1[E2]
9) Chat-Mon	Pn[E2] + Va	->	(1-f).Dn + f.Dn= + P1[Va]
10) Chat-Mon	Pn[Va] + E2	->	(1-f).Dn + f.Dn= + P1[E2]
11) Chat-Mon	Pn[Va] + Va	->	(1-f).Dn + f.Dn= + P1[Va]
12) Chat-Agent	Pn[E2] + Cta	->	Dn + R*
13) Chat-Agent	Pn[Va] + Cta	->	Dn + R*
14) Term-Dis	Pn[E2] + Pm[E2]	->	Dn + (1-f).Dm + f.Dm=
15) Term-Dis	Pn[E2] + Pm[Va]	->	Dn + (1-f).Dm + f.Dm=
16) Term-Dis	Pn[Va] + Pm[E2]	->	Dn + (1-f).Dm + f.Dm=
17) Term-Dis	Pn[Va] + Pm[Va]	->	Dn + (1-f).Dm + f.Dm=
18) Term-Comb	Pn[E2] + Pm[E2]	->	Dn+m
19) Term-Comb	Pn[E2] + Pm[Va]	->	Dn+m
20) Term-Comb	Pn[Va] + Pm[E2]	->	Dn+m
21) Term-Comb	Pn[Va] + Pm[Va]	->	Dn+m
22) Chat-Pol	Pn[E2] + Dm	->	Dn Pm[E2]
23) Chat-Pol	Pn[E2] + Dm	->	Dn Pm[Va]
24) Chat-Pol	Pn[Va] + Dm	->	Dn Pm[Va]
25) Chat-Pol	Pn[Va] + Dm	->	Dn Pm[E2]
26) B-Scission	Pn[E2]	->	(1-f).Dn + f.Dn= + R*
27) B-Scission	Pn[Va]	->	(1-f).Dn + f.Dn= + R*
28) Sc-Branch	Pn[E2]	->	Pn[E2]
29) Sc-Branch	Pn[Va]	->	Pn[Va]

Figure 4.60 Free radical polymerization reactions to produce EVA copolymer

4.6.6 Specifications of Inlet Process Streams, and Unit Operation and Reactor Blocks

Table 4.12 gives the stream and block specifications.

Table 4.12 Stream and block specifications

Stream	Temp °C	Pressure Bar	E2 kg/hr	VA kg/hr	TBPEH kg/hr	CTA Kg/hr	Solvent Kg/hr	Water Kg/hr
C2VAFEED	100	2020	70000	30000				
INITR1	0	2010			50	5	5	
INITR2	0	2010			50	5	5	
CW1, CW2 CW3, CW4	30	100						160000
Block	Temp, °C	Pressure, Bar	Specifications					
HEATER1	250	-10	Liquid-only					
HEATER2	250	-10	Liquid-only					
MIX1, MIX2		2000(MIX1) 1900(MIX2)	Liquid-only					
RPLUG1 RPLUG2 RPLUG3 RPLUG4	Reactor with countercurrent thermal fluid @170°; length = 250 m (RPLUG1 and RPLUG3); 220 m (RPLUG2 and RPLUG4); diameter =0.059 m; pressure drop = 100 bar (process stream); 4 bar (thermal fluid); reaction set = R1							
HPS, LPS	250 bar (HPS); 1 bar (LPS)				Adiabatic, Q = 0 kcal/hr; vapor and liquid phases			

Following Figure 4.43, we specify in the block option of each RPLUG reactor with external thermal fluid (cooling water) the use of steam table, STEAM-A, as the property method for the coolant stream. We also follow Figures 4.44 to 4.46 in Section 4.5.7 to specify the use of the same user subroutine for heat-transfer calculations. We save the simulation file with the initial kinetic parameters as **WS4.3BaseCase.bkp**.

4.6.7 Base-Case Simulation Targets and Kinetic Parameter Estimation

Running the base-case simulation file gives an EVA copolymer production rate of 70,112 kg/hr (which represents a monomer conversion of 70.1%), a MWN of 2385, and a MWW of 980,352.

We apply the methodology for kinetic parameter estimation for LDPE process in Figure 4.26 to EVA copolymerization. According to Table 4.10, the monomer conversion for EVA copolymerization is about 25 to 35%, but it could go up to nearly 40%. We wish to fine-tune our kinetic parameters to produce an **EVA copolymer with a monomer conversion of 39%, a MWN of 49,500 and a MWW of 420,000**.

In particular, we note three important guidelines from Section 4.4.8: (1) as the pre-exponential factors for chain initiation and for chain propagation increase, the production rate or monomer conversion increases; (2) as the pre-exponential factors for chain transfer to monomer, to chain transfer agent or to solvent, and for beta-scission reaction increase, MWN decreases; and (3) as the pre-exponential factor for chain transfer to polymer decreases, MWW (or PDI) decreases.

Following guideline (1), we adjust the pre-exponential factors for chain initiation and propagation, as shown in Figure 4.61, keeping in mind that the propagation pre-exponential factor, $k_{o,E2,E2} = 1.09 * k_{o,E2,VA}$ (that is, $1.635E7 = 1.09 * 1.5E7$ in Figure 4.61), and $k_{o,VA,VA} = 1.06 * k_{o,VA,E2}$ (that is, $1.59E7 = 1.06 * 1.5E7$ in Figure 4.61), according to reference [7] noted in Table 4.10. We set the pre-exponential factors for chain transfer reactions to 12,000. We do not change the pre-exponential factors for other reactions not shown in Figure 4.61. We save the simulation file as **WS4.3-1.bkp**.

Running the simulation file **WS4.3-1.bkp** gives an EVA copolymer production rate of 39141 kg/hr (representing a monomer conversion of 39.1%), and a MWN of 1585 and a MWW of 650,753. The resulting conversion is within the target value between 38 to 40%.

Type	Comp 1	Comp 2	Pre-Exp 1/sec	Act-Energy cal/mol
INIT-DEC	TBPEH		0.00011742	27579.5
CHAIN-INI	E2		1.5e+07	7550.6
CHAIN-INI	VA		1.5e+07	4947.6
PROPAGATION	E2	E2	1.635e+07	7550.6
PROPAGATION	E2	VA	1.5e+07	7550.6
PROPAGATION	VA	E2	1.5e+07	4947.6
PROPAGATION	VA	VA	1.59e+07	4947.6
CHAT-MON	E2	E2	12000	9998.6
CHAT-MON	E2	VA	12000	9998.6
CHAT-MON	VA	E2	12000	6298.8
CHAT-MON	VA	VA	12000	6298.8

Figure 4.61 Modified kinetic parameters to achieve a monomer conversion between 38% to 40%.

Following guidelines (2) and (3) for kinetic parameter tuning, we increase the pre-exponential factor for chain transfer to monomer and to agent from 12,000 to 16,400, change the pre-exponential factor for beta scission to also 16,400, and decrease the pre-exponential factor for chain transfer to polymer to 2.44E5. Table 4.13 shows the resulting comparison of simulation results with target values. We save the simulation file as **WS4.3-2.bkp**.

Table 4.12 Comparison of simulation results with production targets

	Target	Simulation	Error %
EVA copolymer, kg/hr	39,000	38,949	0.131%
MWN	49,500	49,606.2	0.2%
MWW	420,000	420,357	0.0085%

This chapter is published with Wiley publication in the book *Integrated Process Modeling, Advanced Control and Data Analytics for Optimizing Polyolefin Manufacturing* by Liu & Sharma.[39-50]

4.7 Bibliography

1. Odian, G. (1991). *Principles of Polymerization*, 3rd edition, Wiley, New York.
2. Aspen Technology, Inc. (2017). Free Radical Bulk Polymerization Models. *Aspen Polymers V8.5 Unit Operation and Reactor Models*, pp. 163-198.
3. Aspen Technology, Inc. (2017). Initiator Decomposition Rate Parameters. *Aspen Polymers V8.5 Unit Operation and Reactor Models*, pp. 431-44.
4. Hui, A. W.; Hamielec, A. E. (1972). Thermal Polymerization of Styrene at High Conversions and Temperatures: An Experimental Study. *J. Appl. Polym. Sci.*, **16**, 749.
5. Author unknown, Chapter 1: Free Radical Polymerization, https://ethz.ch/content/dam/ethz/special-interest/chab/icb/morbidelli-dam/documents/Education/PRCE/DOC_2016/Chapter1.pdf, accessed June 8, 2020.
6. Kan, T. W. (2003). Modeling of High-Pressure Ethylene-Vinyl Acetate Copolymer in Autoclave Reactor. M.S. thesis, Department of Chemical Engineering, National Taiwan University of Science and Technology, Taipei.
7. Ratzsch, M., Schneider, W., Musche, D. (1971). Reactivity of Ethylene in the Radically Initiated Copolymerization of Ethylene with Vinyl Acetate. *J. Poly. Sci. Part A-1*, **9**, 785.
8. Bokis, C. P.; Orbey, H.; and Chen, C. C. (1999). Properly Model Polymer Processes. *Chem. Eng. Prog.*, **95**, No. 4, 39.
9. Aspen Technology, Inc. (2019), *Aspen Physical Property System: Physical Property Models, V.11*.
10. Sanchez, I. C.; Lacombe, R. H. (1978). Statistical Thermodynamics of Polymer Solutions. *Macromolecules*, **11**, 1145.
11. Orbey, H., Bokis, C. P., Chen, C. C. (1998). Equation of State Modeling of Phase Equilibrium in the Low-Density Polyethylene Process: The Sanchez–Lacombe, Statistical Associating Fluid Theory, and Polymer-Soave–Redlich–Kwong Equations of State. *Ind. Eng. Chem.*, **37**, 4481.
12. Aspen Technology, Inc. (2017). Application B1 - Polystyrene Bulk Polymerization by Thermal Initiation. *Aspen Polymers V8.4: Examples and Applications*, pp. 97-108.

13. Yan, R., Study of Operating Mode and Process Simulation of LDPE Plant at BYPC. (2000)., *China Synthetic Resin and Plastics*, **17**, No. 2, 36.
14. Aspen Technology, Inc. (2017). Application B8 - Low-Density High-Pressure Process. *Aspen Polymers V8.4: Examples and Applications*, pp. 187-204.
15. Kiparissides, C., Veros, G., MacGregor, J. F. (1993). Mathematical Modeling, Optimization, and Quality Control of High-Pressure Ethylene Polymerization Reactor. *Rev. Macromol. Chem. Phys.* **C33**, 437.
16. Gross, J., Sadowski, G. (2001). Perturbed-Chain SAFT: An Equation of State Based on a Perturbation Theory for Chain Molecules. *Ind. Eng. Chem. Res.*, **40**, 1244.
17. Gross, J., Sadowski, G. (2002). Application of Perturbed-Chain SAFT Equation of State to Associating Systems. *Ind. Eng. Chem. Res.*, **41**, 5510.
18. Bokis, C. P., Ramanathan, S., Franjione, J., Buchelli, A., Call, M. L., Brown, A. L. (2002). Physical Properties, Reactor Modeling, and Polymerization Kinetics in the Low-Density Polyethylene Tubular Reactor Process. *Ind. Eng. Chem. Res.*, **41**, 1017.
19. Cheluget, E. L., Bokis, C. P., Wardhagh, L., Chen, C. C., Fisher, J. (2002). Modeling Polyethylene Fractionation Using the Perturbed-Chain Statistical Associating Fluid Theory Equation of State. *Ind. Eng. Chem. Res.*, **41**, 968.
20. Chen, C. H., Vermeuchuk, Howell, J. A., Ehrlich, P. (1976). Computer Model for Tubular High-Pressure Polyethylene Reactor. *AIChE J.*, **22**, 463.
21. Hendrickson, G. (1997). Simulation of a LDPE Autoclave Reactor with POLYMERS PLUS. Presented at Aspen World, Boston, MA, Oct., 1997. See: <https://docplayer.net/27596341-Simulation-of-a-ldpe-autoclave-reactor-with-polymers-plus-greg-hendrickson-senior-process-engineer-chevron-chemical-company-kingwood-texas.html>. Accessed May 20, 2020.
22. Caliani, E., Cavalcanti, M., Lona, L. M., Fernandez, F. (2008). Modeling and Simulation of High-Pressure Industrial High-Pressure Polyethylene Reactor. *eXpress Polymer Letters*, **2**, 57.
23. Azmi, A., Aziz, N. (2016). Low Density Polyethylene Tubular Reactor Modeling: Overview of the Model Developments and Future Directions. *J. Applied Engineering Research*, **11**, 9906.
24. Zhmad, Z., Azix, N. (2018). Modeling and Nonlinearity of Low-Density Polyethylene (LDPE) Tubular Reactor. *Materials Today: Proceedings*, **5**, 21612.
25. Pladis, P., Kiparissides, C. (2014). Polymerization Reactors. <https://doi.org/10.1016/B978-0-12-409547-2.10908-4>. Accessed June 1, 2020.
26. Camacho, J., Diez, E., Diaz, I., Ovejero, G. (2017). PC-SAFT Thermodynamics of EVA Copolymer-Solvent Systems., *Fluid Phase Equilibria*, **449**, 10.
27. Kawahara, T., Hikasa, T. (2005). Method for Producing Ethylene-Vinyl Acetate Copolymer and Saponified Product Thereof., U. S. Patent 6,838,517 B2.
28. Lee, Y., Jeon, K., Cho, J., Na, J., Park, J., Jung, I. Park, J., Park, M. J., Lee, W. B. (2019). Multicomponent Model of Ethylene-Vinyl Acetate Autoclave Reactor: A Combined Computational Fluid Dynamics and Polymerization Kinetics Model. *Ind. Eng. Chem. Res.*, **58**, 16459.

29. Samaroria, C., Brandolin, A. (2000), Modeling of Molecular Weights in Industrial Autoclave Reactors for High Pressure Polymerization of Ethylene and Ethylene-Vinyl Acetate. *Polymer Engineering and Science*, **40**, 1480.
30. Ghiass, M., Hutchinson, R. A. (2003). Simulation of Free Radical High Pressure Copolymerization in a Multizone Autoclave: Model Development and Application. *Polymer Reaction Engineering*. **11**, 989.
31. Chien, I. L., Kan, T. W., Cheb, B. S. (2007). Dynamic Simulation and Operation of a High Pressure Ethylene-Vinyl Acetate Autoclave Reactor. *Computers and Chem. Eng.*, **31**, 233.
32. Chen, B. S. (2004). Modeling and Control of High-Pressure Ethylene-Vinyl Acetate Copolymerization Process. M.S. thesis, Department of Chemical Engineering, National Taiwan University of Science and Technology, Taipei.
33. Lee, H. Y., Yang, T. H., Chien, I. L., Huang, H. P. (2009). Grade Transition Using Dynamic Neural Networks for an Industrial High-Pressure Ethylene-Vinyl Acetate (EVA) Copolymerization Process. *Computers Chem. Eng.*, **33**, 1371.
34. Sharmin, R., Sundararaj, U., Shah, S., Griend, L. V., Sun, Y. J. (2006). Inferential Sensors for Estimation of Polymer Quality Parameters: Industrial Application of PLS-Based Soft Sensor for a LDPE Plant. *Chem. Eng. Sci.*, **61**, 6372.
35. Chien, I. L., Kan, T. W. and Chen, B. S. (2005). Rigorous Modeling of a High-Pressure Ethylene-Vinyl Acetate (EVA) Copolymerization Autoclave Reactor. IFAC Proceedings; see <https://folk.ntnu.no/skoge/prost/proceedings/ifac2005/Fullpapers/02171.pdf>. Accessed June 10, 2020.
36. Aspen Technology, Inc. (2017). Application B4 – Styrene Ethyl Acrylate Free Radical Copolymerization Process. *Aspen Polymers V8.4: Examples and Applications*, pp. 133-146.
37. López-Carpy, B., Saldívar-Guerra, E., Zapata-González, I. and García-Franco, C. (2018). Mathematical Modeling of the Molecular Weight Distribution in Low Density Polyethylene. I. Steady-State Operation of Multizone Autoclave Reactors. *Macromolecular Reaction Engineering*, **12**, 1800013.
38. Liu, Y. L., Su, G. R., Cheng, M. H. (2019). The Comparison and Prospect of EVA Plant with Tubular Reactor and Autoclave Reactor. *Zhejiang Chemical Industry*, **50**, No. 7, 29.
39. Liu, Y. A., & Sharma, N. (2023). *Integrated Process Modeling, Advanced Control and Data Analytics for Optimizing Polyolefin Manufacturing*. Wiley-VCH GmbH (<https://doi.org/10.1002/9783527843831>)
40. Liu, Y. A., & Sharma, N. (2023). Introduction to Integrated Process Modeling, Advanced Control, and Data Analytics in Optimizing Polyolefin Manufacturing. In *Integrated Process Modeling, Advanced Control and Data Analytics for Optimizing Polyolefin Manufacturing* (Chapter 1, pp. 1-40). Wiley-VCH GmbH. <https://doi.org/10.1002/9783527843831.ch1>
41. Liu, Y. A., & Sharma, N. (2023). Selection of Property Methods and Estimation of Physical Properties for Polymer Process Modeling. In *Integrated Process Modeling, Advanced Control and Data Analytics for Optimizing Polyolefin Manufacturing* (Chapter 2, pp. 41-86). Wiley-VCH GmbH. <https://doi.org/10.1002/9783527843831.ch2>

42. Liu, Y. A., & Sharma, N. (2023). Reactor Modeling, Convergence Tips, and Data-Fit Tool. In *Integrated Process Modeling, Advanced Control and Data Analytics for Optimizing Polyolefin Manufacturing* (Chapter 3, pp. 87-114). Wiley-VCH GmbH. <https://doi.org/10.1002/9783527843831.ch3>

43. Liu, Y. A., & Sharma, N. (2023). Free Radical Polymerizations: LDPE and EVA. In *Integrated Process Modeling, Advanced Control and Data Analytics for Optimizing Polyolefin Manufacturing* (Chapter 4, pp. 115-162). Wiley-VCH GmbH. <https://doi.org/10.1002/9783527843831.ch4>

44. Liu, Y. A., & Sharma, N. (2023). Ziegler–Natta Polymerization: HDPE , PP , LLDPE, and EPDM. In *Integrated Process Modeling, Advanced Control and Data Analytics for Optimizing Polyolefin Manufacturing*. (Chapter 5, pp. 163-265). Wiley-VCH GmbH. <https://doi.org/10.1002/9783527843831.ch5>

45. Liu, Y. A., & Sharma, N. (2023). Free Radical and Ionic Polymerizations: PS and SBS Rubber. In *Integrated Process Modeling, Advanced Control and Data Analytics for Optimizing Polyolefin Manufacturing*. (Chapter 6, pp. 267-319). Wiley-VCH GmbH. <https://doi.org/10.1002/9783527843831.ch6>

46. Liu, Y. A., & Sharma, N. (2023). Improved Polymer Process Operability and Control Through Steady-State and Dynamic Simulation Models. In *Integrated Process Modeling, Advanced Control and Data Analytics for Optimizing Polyolefin Manufacturing*. (Chapter 7, pp. 321-379). Wiley-VCH GmbH. <https://doi.org/10.1002/9783527843831.ch7>

47. Liu, Y. A., & Sharma, N. (2023). Model-Predictive Control of Polyolefin Processes. In *Integrated Process Modeling, Advanced Control and Data Analytics for Optimizing Polyolefin Manufacturing*. (Chapter 8, pp. 381-476). Wiley-VCH GmbH. <https://doi.org/10.1002/9783527843831.ch8>

48. Liu, Y. A., & Sharma, N. .2023. Application of Multivariate Statistics to Optimizing Polyolefin Manufacturing. In *Integrated Process Modeling, Advanced Control and Data Analytics for Optimizing Polyolefin Manufacturing* (Chapter 9, pp. 477-531). Wiley-VCH GmbH. <https://doi.org/10.1002/9783527843831.ch9>

49. Liu, Y. A., & Sharma, N. (2023). Applications of Machine Learning to Optimizing Polyolefin Manufacturing. In *Integrated Process Modeling, Advanced Control and Data Analytics for Optimizing Polyolefin Manufacturing*. (Chapter 10, pp. 553-650). Wiley-VCH GmbH. <https://doi.org/10.1002/9783527843831.ch10>.

50. Liu, Y. A., & Sharma, N. (2023). A Hybrid Science-Guided Machine Learning Approach for Modeling Chemical and Polymer Processes. In *Integrated Process Modeling, Advanced Control and Data Analytics for Optimizing Polyolefin Manufacturing*. (Chapter 11, pp. 651-698). Wiley-VCH GmbH. <https://doi.org/10.1002/9783527843831.ch11>
